Jean Francois Van Huele
Feb 2000

A STUDY OF QUANTUM CLOCKS

by

Seokjae Kim

A thesis submitted to the faculty of

Brigham Young University

in partial fulfillment of the requirements for the Degree of

Master of Science

Department of Physics and Astronomy

Brigham Young University

December 1999

BRIGHAM YOUNG UNIVERSITY

GRADUATE COMMITTEE APPROVAL

of a thesis submitted by

Seokjae Kim

This thesis has been read by each member of the following graduate committee and by majority vote has been found to be satisfactory.

11/30/1999	Jean-François Van Huele, Chair
Date	
11/30/1999	Manuel Berrondo
Date	
11/30/1999	William E. Dibble
Date	
12/3/99	William E. Evenson
Date	

BRIGHAM YOUNG UNIVERSITY

As chair of the candidate's graduate committee, I have read the thesis of Seokjae Kim in its final form and have found that (1) its format, citations, and bibliographical styles are consistent and acceptable and fulfill university and department style requirements; (2) its illustrative materials including figures, tables, and charts are in place; and (3) the final manuscript is satisfactory to the graduate committee and is ready for submission to the university library.

11/30/1999
Date

Jean-François Van Huele
Chair, Graduate Committee

Accepted for the Department

Dorian M. Hatch
Department Chair

Accepted for the College

Nolan Mangelson
Associate Dean, College of Physical and Mathematical Sciences

ABSTRACT

A STUDY OF QUANTUM CLOCKS

Seokjae Kim

Department of Physics and Astronomy

Master of Science

In the microscopic domain, time measurements are obtained by applying quantum operators called quantum clocks. We review different types of quantum clocks, based on a time-independent Hamiltonian. Explicit microscopic models of ticking quantum clocks are constructed by using the superposition of wavefunctions in periodic multi-wells. Dispersion of the wave packet and accuracy of the clocks are discussed. The transition to relativistic clocks is addressed and some solutions for the relativistic double well are presented.

Contents

List of Figures

Chapter 1

Introduction to Time

1.1 What is Time?

Time is one of the dimensions in which we are conscious of the world. However, the true character of time is not easily grasped thoroughly. In his *Confessions* St. Augustine said, "What is time?—if nobody asks me, I know; but if I try to explain it to one who asks me, I do not know" [10]. Human beings have been pondering to find the character of time for a time as long as their history. One central concern of Greek, Oriental and Western philosophy was about the concepts of time in eternity and transience. Although the Greek philosophers developed systematic geometry, they could not figure out the answer about the concept of time because the answer lay beyond pure mathematics. Aristotle discovered a fundamental role for time by

studying the motion in time, but he failed to introduce the notion of time as an 'abstract parameter of mathematics' [6]. Time was motion to him and he perceived time through the motion of objects.

The concept of time as an independently existing entity emerged in Europe during the medieval era. The existence of an order in nature was recognized and a precise and objective meaning was given to that order with the rise of modern science. For this purpose clocks were designed to tell the time, and to organize human activities.

It was Galileo who transformed time to a practical, measurable quantity after watching a swinging lamp in a church. By measuring the period of the swing against the pulse of his wrist, he discovered the law of the pendulum. It did not take long until Huygens built the pendulum clock.

More than ever the subject of time is central to all of us. We can only feel what time means from our daily experience in which time is appointments, transportations, business and class schedules, television programs, and cooking controls. Of course, it is by no means obvious in all these cases what time is exactly. However, in these experiences time involves at least the following characteristics: (1)an irreversible one-way direction, (2)categorical differences between past, present and future, and (3)constant becoming [10]. It is sometimes stated that physics provides no basis for any of these

features. But for physicists there is no other way to solve the problem of time than through physics. Hans Reichenbach said, "if time is objective, the physicist must have discovered the fact; if there is Becoming, the physicist must know it; if there is a solution to the philosophical problem of time, it is written down in the equations of mathematical physics" [10]. There is a vast literature on the meaning of time and on the perception of time through history. We refer the reader to source references [6, 10, 20, 21, 22, 23] on time both within and outside of physics.

1.2 Time in Physics

Time in physics is different from time in philosophy or psychology. It is defined by the way it enters the metaphysical structure of any particular physical theory. We do not assert that physical theories can ultimately solve the metaphysical problems that time raises. Physics is mainly concerned with the measurement of time, rather than with the essentially metaphysical questions as to its nature. Accurate measurement of time is a practical and fundamental task for physicists.

To measure time in classical mechanics, we actually have to observe some dynamical variables and use the laws of motion. We do not assign time to a particle like we do mass or charge. In Schrödinger's theory time is not a dynamical variable but a parameter, so that it is not an observable. Therefore, the measurement of time

is different from that of other quantities such as position, energy, or momentum.

Before Galileo and Newton, time was just an abstract thing, not a parameter to be measured with geometrical precision. Time was a part of nature. Newton, however, took time right out of nature and gave it an independent existence. He made time part of the laws of the universe in the late seventeenth century. By his work time entered into the laws of mechanics and it became a fundamental parameter in the physical world. His time is an absolute, true and mathematical time. It existed independently of the human mind and flowed without relation to the external world with which it interacted. He made time an exactly measurable dimension, but his time taught us little about time itself because his time acted merely as a way to keep track of motion mathematically.

Leibniz had different views of space and time from Newton. To Newton space and time were absolute and real entities. They existed independently of the human mind. This has now come to be called 'classical physics.' He felt that if they were absolute and real, they would be independent of God and set limitations on God's capabilities; that is, God would not be able to exert any control over them. For him space and time were orders or relations. Whereas space is the "order of coexistences," time is the "order of successions" [11]. His view was essentially relativistic. It took two centuries for physicists to catch up with these relativistic views of Leibniz.

The story of time in the twentieth century is overwhelmingly the story of Einstein. He, more than anyone else, is responsible for time being a measurable quantity. He restored time to its right place at the core of nature, as one of the four dimensions of space-time. Relativity was a monumental first step towards the rediscovery of time. His time was intrinsically flexible and tied to the experience of an individual observer. Thus, in special relativity his time is called the 'proper time' which is the time in the reference frame where two events occur at the same place.

Although the relativity of motion was known to Galileo, what Einstein rediscovered was that not only motion but also space and time were relative. His work revolutionized our understanding of time, but the consequences, especially the implications on time from general relativity and cosmology, have yet to be fully worked out. Beyond his work scientists probed deeper and deeper into the mysteries of time by asking questions concerning the beginning and the end of time, the directionality of time, and the possibility of time travel, etc. In spite of nearly a century of investigation, we have not yet found clear answers to any one of these questions. Even Einstein's time is probably inadequate to explain fully the physical universe and our conception of it. A revolution was started by Einstein, but it remains unfinished.

The other big revolution in twentieth century science is quantum theory. Like relativity, quantum theory forced us to change our understanding of the universe. The

well as the time operator of the quantum clock. In Chapter 4 I will explore various symmetric square well potentials to construct an explicit model for a ticking quantum clock. In addition, I will discuss the accuracy and dispersion of the quantum clock. In Chapter 5 I will study relativistic single and double square well potentials as a first model for a clock whose inner working is represented by a relativistic microsystem. Finally, in Chapter 6 I will describe some limitations on constructing real quantum clocks.

Chapter 2

Background on Quantum Clocks

In this chapter I will discuss the general properties of a quantum clock and describe two models of quantum clocks that of Salecker and Wigner and that of Peres.

2.1 What is a Quantum Clock?

To measure time in quantum mechanics, we use a quantum clock. A time-independent Hamiltonian has to be introduced. The idea of the quantum clock came from the possibility that we might describe the measurement of time in a 'realistic' way by the clock mechanism in the time-independent Hamiltonian. Then quantum time can be registered simply in terms of the distance or the position of a particle if we assume that we know what the position of the particle is.

apparatus, we have

$$t\,\Delta E\,\Delta Q \geq \frac{\hbar}{2} t \left| \frac{d\langle Q \rangle}{dt} \right| \geq \frac{\hbar}{2} \Delta Q. \tag{2.3}$$

Thus, if the clock is to serve its purpose, whatever Q may be, t must satisfy

$$t\,\Delta E \geq \frac{\hbar}{2}, \tag{2.4}$$

where ΔE is the energy uncertainty of the system's state.

2.2 Salecker and Wigner's Quantum Clock

H. Salecker and E. P. Wigner first introduced the quantum clock in 1958 [19]. The clock is composed of N potential wells in which one particle is confined. Then the wave function of the clock, ψ, is the superposition of N stationary states $\phi_1, \phi_2, \ldots, \phi_N$ and the potential has very closely spaced energy levels. If the clock has an accuracy τ, the wave function ψ will actually go through N orthogonal states at time $\tau, 2\tau, \ldots, N\tau$, and the location of the particle will change from one trough to the other. The location of the particle indicates the pointer of the clock, and the clock measures the maximum time interval $T = N\tau$, which is the proper time for the system. The clock registers intervals of time by obeying quantum mechanics.

Salecker and Wigner focused on the intrinsic quantum limitations imposed on the measurement of space-time distances. They proposed to use only clocks for the

record of the physical processes that it had monitored.

His model of the clock is similar to the usual round-shaped mechanical clock we can see around us. From the wave functions of the clock and orthogonal basis for them, a sharp peak happens at $\theta = \frac{2\pi k}{N}$, where θ is the angular position of the sharp peak on the clock, N is the number of states or the total number of hours the clock indicator points, and $k = 0, 1, \ldots, N-1$. The sharp peak is said to point to the 'kth' hour. Then he introduced a projection operator and a clock time operator of which an eigenvector is the 'kth' orthogonal basis of the clock wave functions and an eigenvalue is $k\tau$. This yields at best a discrete approximation to the true time by measuring the clock time operator. It is by the time independent Hamiltonian of the clock that a clock successively passes through the states $\phi_0, \phi_1, \phi_2, \ldots$ at every time interval τ.

Chapter 3

Study of Nonrelativistic Quantum Clocks

In this chapter I will discuss non-relativistic quantum clocks. The Hamiltonian of the quantum clock as well as the time operator of the quantum clock will be introduced and it will be shown how the wavefunction of the quantum clock evolves.

3.1 The Wave Function of the Quantum Clock

The quantum clock of Peres's model can be described as follows [18]. The wave function ψ of the quantum clock is

$$\psi_m(\theta) = \frac{1}{\sqrt{2\pi}} e^{im\theta} \tag{3.1}$$

and $t_k = k\tau$ is a discrete approximation to the true time (it is assumed that the initial state of the clock is always ϕ_0).

3.3 The Hamiltonian of the Quantum Clock

The Hamiltonian is an energy operator in quantum mechanics. The Hamiltonian of the quantum clock can be written as

$$H_c = \omega J, \tag{3.6}$$

where $\omega = \frac{2\pi}{N\tau}$ and $J = -i\hbar\frac{\partial}{\partial\theta}$. If it is applied to the quantum clock wavefunction, the eigenvalue equation is

$$H_c\psi_m = m\hbar\omega\psi_m, \tag{3.7}$$

and the quantum system evolves as time goes by

$$e^{-iH_ct/\hbar}\,\psi_m = e^{-im\omega t}\,\psi_m = \frac{1}{\sqrt{2\pi}}e^{im(\theta-\omega t)}. \tag{3.8}$$

3.4 The Evolution of the Quantum Clock

The evolution is given by

$$e^{-iH_ct/\hbar}\,\phi_k = \phi_{k+1}, \tag{3.9}$$

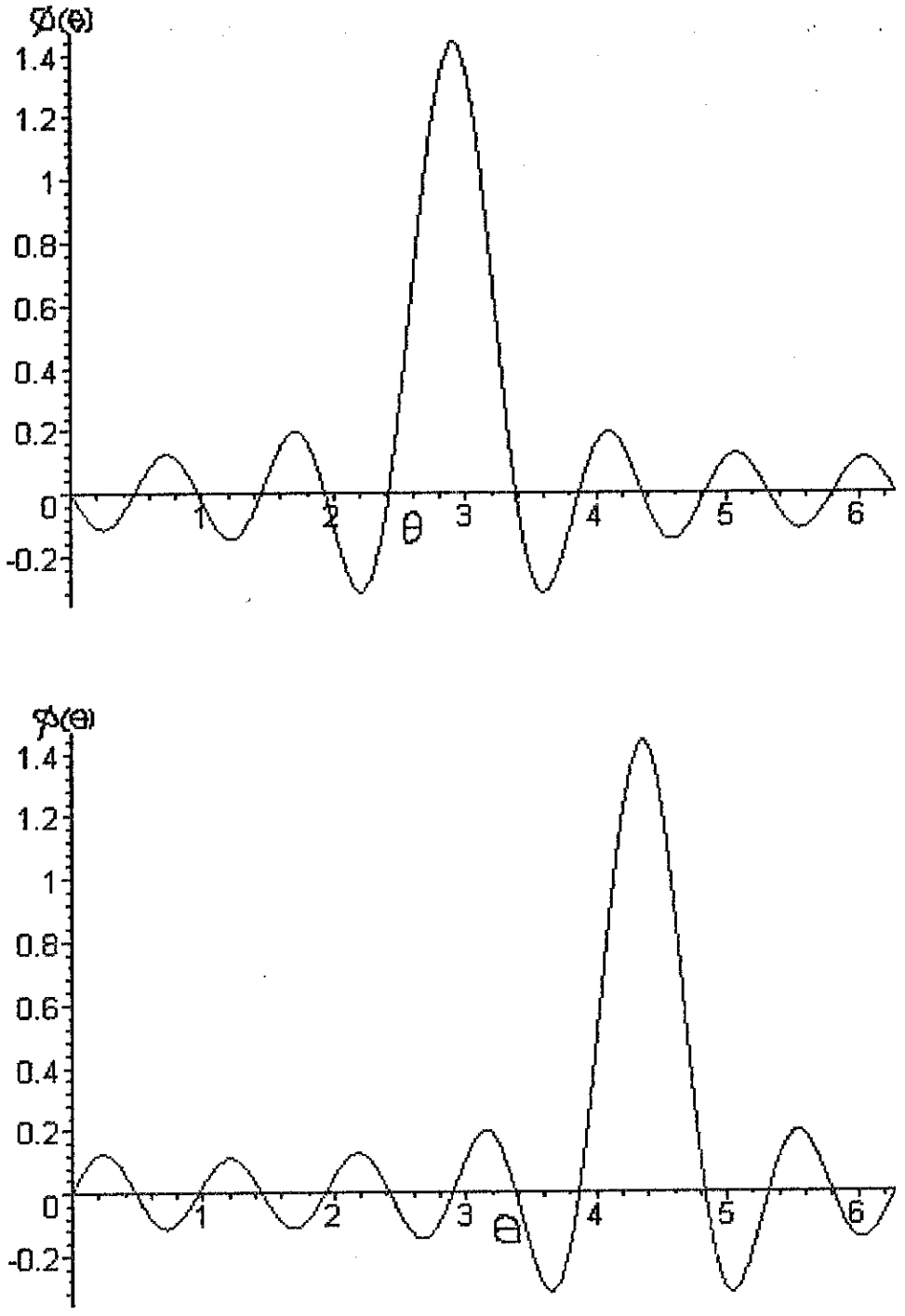

Figure 3.2: The sharp peaks of $\phi_k(\theta)$ occurring in Peres's quantum clock. $N = 13$, $k = 6$ (top) and $k = 9$ (bottom).

Chapter 4

An Explicit Model for a Ticking Quantum Clock

In this chapter I will explore the various symmetric square well potentials to construct an explicit model for a ticking quantum clock. In addition, I will discuss the accuracy and dispersion of the quantum clock. An explicit model for a ticking quantum clock can be constructed with a one-dimensional periodic well potential of which the total width is L as shown in Figure 4.1 as first proposed by Salecker and Wigner [19]. We choose a potential consisting of N very narrow wells and $N-1$ equally narrow barriers. The potential energy is infinite at both end walls and alternates between zero and V_0 in between. It confines a particle between the two end walls and

has a lot of very closely spaced energy levels clustered in groups of N as shown in Figure 4.2. I will consider a very special superposition of these levels in Section 4.5.

If the constants of the system are properly adjusted in such a way that the level spacing becomes $\frac{\hbar}{T}$, where T is a maximum time interval T, the time dependent wavefunction ψ can be chosen as

$$\psi(t) = \sum_{1}^{N} a_k \, \phi_k \, e^{-i\omega_k t} \tag{4.1}$$

where the constant $a_k = \frac{1}{\sqrt{N}}$ is a normalization factor and ω_k can be expressed as

$$\omega_k = \omega_0 + \frac{2\pi k}{N\tau} = \omega_0 + \frac{2\pi k}{T}. \tag{4.2}$$

The wavefunction will have the property that the position of the particle changes, in the time element τ, from one trough to the next (from left to right). After N such transitions and a time $N\tau = T$, the particle finds itself in the right-most trough. This is the maximal time for the clock to go once around.

We can also see that the clock now evolves periodically because at an arbitrary time t the clock wavefunction is

$$\begin{aligned} \psi(t) &= \frac{1}{\sqrt{N}} \left(\phi_1 e^{-i\omega_1 t} + \phi_2 e^{-i\omega_2 t} + \cdots + \phi_N e^{-i\omega_N t} \right) \\ &= \frac{e^{-i\omega_0 t}}{\sqrt{N}} \left(\phi_1 e^{-i\frac{2\pi}{N\tau}t} + \phi_2 e^{-i\frac{4\pi}{N\tau}t} + \cdots + \phi_N e^{-i\frac{2\pi}{\tau}t} \right) \end{aligned} \tag{4.3}$$

and for each time interval τ, $2\tau, \ldots, N\tau$,

$$\psi(\tau) = \frac{e^{-i\omega_0 t}}{\sqrt{N}}\left(\phi_1 e^{-i\frac{2\pi}{N}} + \phi_2 e^{-i\frac{4\pi}{N}} + \cdots + \phi_N e^{-i2\pi}\right) \tag{4.4}$$

$$\psi(2\tau) = \frac{e^{-i\omega_0 t}}{\sqrt{N}}\left(\phi_1 e^{-i\frac{4\pi}{N}} + \phi_2 e^{-i\frac{8\pi}{N}} + \cdots + \phi_N e^{-i4\pi}\right) \tag{4.5}$$

$$\vdots$$

$$\psi(N\tau) = \frac{e^{-i\omega_0 t}}{\sqrt{N}}\left(\phi_1 e^{-i2\pi} + \phi_2 e^{-i4\pi} + \cdots + \phi_N e^{-i2N\pi}\right) \tag{4.6}$$

and for $t = (N+1)\tau$

$$\begin{aligned}\psi(N\tau+\tau) &= \frac{e^{-i\omega_0 t}}{\sqrt{N}}\left(\phi_1 e^{-i\frac{2\pi}{N}(N+1)} + \phi_2 e^{-i\frac{4\pi}{N}(N+1)} + \cdots + \phi_N e^{-i2\pi(N+1)}\right)\\ &= \frac{e^{-i\omega_0 t}}{\sqrt{N}}\left(\phi_1 e^{-i\frac{2\pi}{N}} + \phi_2 e^{-i\frac{4\pi}{N}} + \cdots + \phi_N e^{-i2\pi}\right)\\ &= \psi(\tau).\end{aligned} \tag{4.7}$$

Thus, the period of the clock is $T = N\tau$, and at $t = (N+1)\tau$ the indicator of the clock points the same position as that at $t = \tau$. In this way, the position of the particle can be considered as the pointer of the clock.

4.1 Symmetric Double Well Potential

In this section I construct the explicit solution in the special case of a double well potential. Let's consider the stationary solution of the potential shown in Figure

4.3 for $E \leq V_0$. This one dimensional double well potential is symmetric with respect to reflection around its central y-axis. The width of each of the potential well is labeled a and that of the central barrier is labeled b. We distinguish three regions from left to right, 'Region I,' 'Region II,' and 'Region III,' and establish appropriate eigenfunctions in each region:

$$\psi_I(x) = A\,e^{ikx} + B\,e^{-ikx} \tag{4.8}$$

for $-a - b/2 \leq x \leq -b/2$,

$$\psi_{II}(x) = C\,e^{qx} + D\,e^{-qx} \tag{4.9}$$

for $-b/2 \leq x \leq b/2$, and

$$\psi_{III}(x) = F\,e^{ikx} + G\,e^{-ikx} \tag{4.10}$$

for $b/2 \leq x \leq a + b/2$. Here, we define $k = \frac{\sqrt{2mE}}{\hbar}$, and $q = \frac{\sqrt{2m(V_0 - E)}}{\hbar}$ as the real wave numbers in the troughs and barriers.

Symmetric considerations lead to the following simplification. The symmetry of the potential imposes reflection symmetry of the probability density around the central axis. When x is replaced by $-x$, a function $\psi(x)$ needs to exhibit the following property:

$$|\psi(x)|^2 = |\psi(-x)|^2 \tag{4.11}$$

By the symmetric structure of the double well potential, if we replace x with $-x$ in ψ_I, we get ψ_{III} in x, and vice verse. The condition is

$$\psi_I(-x) = A\,e^{ik(-x)} + B\,e^{-ik(-x)} = \psi_{III}(x) = F\,e^{ikx} + G\,e^{-ikx}. \tag{4.18}$$

Because e^{ikx} and e^{-ikx} are linearly independent functions, $A = G$ and $B = F$. Similarly, the antisymmetric solution of the double well potential yields $A = -G$ and $B = -F$.

By doing this we have reduced six coefficients to four. We can further reduce the number of the coefficients to three by imposing the symmetry consideration on the wavefunction in the central barrier

$$\psi_{II}(-x) = \pm\psi_{II}(x). \tag{4.19}$$

This implies $D = \pm C$. We now choose to solve the even and odd solutions separately. In this case we can just set up a 3×3 matrix from the boundary conditions

$$\psi_{III}(a + b/2) = 0 \tag{4.20}$$

$$\psi_{II}(b/2) = \psi_{III}(b/2) \tag{4.21}$$

and at $x = b/2$

$$\frac{d\psi_{II}}{dx} = \frac{d\psi_{III}}{dx}, \tag{4.22}$$

and find its determinant. This determinant expresses the condition on the allowed energy levels since all boundary conditions are to be satisfied simultaneously.

If we do not use the symmetry consideration, we can find both even and odd solutions by solving the determinant of a 6×6 matrix, the final equation is

$$-2kq \sin(2ka) = \tanh(qb)[(k^2 + q^2) + (k^2 - q^2)\cos(2ka)]. \tag{4.23}$$

This equation can be further transformed by choosing $a = b$ (equal width for well and barrier), and defining $\xi = ka$, $\eta = qa$, and $\lambda = \frac{\sqrt{2mV_0}}{\hbar}a$. Then $\lambda^2 = \xi^2 + \eta^2$, and (4.23) can be rewritten as

$$-2\coth\left(\sqrt{\lambda^2 - \xi^2}\right) = \frac{\sqrt{\lambda^2 - \xi^2}}{\xi}\tan(\xi) + \frac{\xi}{\sqrt{\lambda^2 - \xi^2}}\cot(\xi). \tag{4.24}$$

By plotting the left-hand and the right-hand sides of this equation separately, we can find both even and odd solutions together for given λ's and a's. The results are plotted on Figure 4.4. The graph shows that the eigenvalue solutions of these two equations appear paired and they are quasi-degenerate.

On the contrary, we can solve by separating even solutions from odd solutions and solve 3×3 determinants only. We return to the general case where 'a' and 'b' are not necessarily equal each other. For the even states the wave functions in each region can be chosen as

$$\psi_I = A\sin(kx) + B\cos(kx) \tag{4.25}$$

$$\psi_{II} = D\cosh(qx) \tag{4.26}$$

$$\psi_{III} = B\sin(kx) + A\cos(kx). \tag{4.27}$$

By applying boundary conditions we finally get an equation for the energy solutions of the even states as

$$-q \tanh(q\,b/2) = k \cot(ka). \tag{4.28}$$

For the odd states the wave functions in each region are

$$\psi_I = A\sin(kx) + B\cos(kx) \tag{4.29}$$

$$\psi_{II} = C\sinh(qx) \tag{4.30}$$

$$\psi_{III} = -B\sin(kx) - A\cos(kx). \tag{4.31}$$

The final energy solution equation for these states after applying boundary conditions is

$$-q \coth(q\,b/2) = k \cot(ka). \tag{4.32}$$

Particularizing to the case where $a = b$, these even and odd energy solutions can be rewritten respectively as

$$-\cot(\xi) = \frac{\sqrt{\lambda^2 - \xi^2}}{\xi} \tanh\left(\frac{\sqrt{\lambda^2 - \xi^2}}{2}\right) \tag{4.33}$$

$$-\cot(\xi) = \frac{\sqrt{\lambda^2 - \xi^2}}{\xi} \coth\left(\frac{\sqrt{\lambda^2 - \xi^2}}{2}\right) \tag{4.34}$$

where $\xi = ka$, $\eta = qa$, and $\lambda = \frac{\sqrt{2mV_0}}{\hbar}a$. The even and odd energy solutions are plotted in Figure 4.5. As can be seen in Figure 4.5, the even and odd solutions have almost the same values except when the levels are very close to the top of the potential

So

$$\xi = \left(n + \frac{1}{2}\right)\pi = k\,a = \sqrt{\frac{2mE}{\hbar^2}}a. \tag{4.41}$$

Thus,

$$E = \left(n + \frac{1}{2}\right)^2 \frac{\pi^2\hbar^2}{2ma^2} \tag{4.42}$$

where $n = 0, 1, 2, 3, \ldots$.

For the odd case, let $x = \sqrt{\lambda^2 - \xi^2}$. Then

$$\lim_{x\to 0} \frac{x}{\xi} \coth\left(\frac{x}{2}\right) = \frac{1}{\xi}. \tag{4.43}$$

Therefore,

$$-\cot(\xi) = \frac{1}{\xi} \tag{4.44}$$

or

$$-\xi\cot(\xi) = 1. \tag{4.45}$$

We can graphically find the energy states of the odd case for given potential energy and the width of 'a.' Results are presented in Figure 4.6.

Comparing these even and odd solutions, we can see from Figure 4.7 that the even states are slightly below the odd states when $V \geq E$, and the gap between them becomes smaller as the energy increases, and tends to be zero as the barrier becomes infinite.

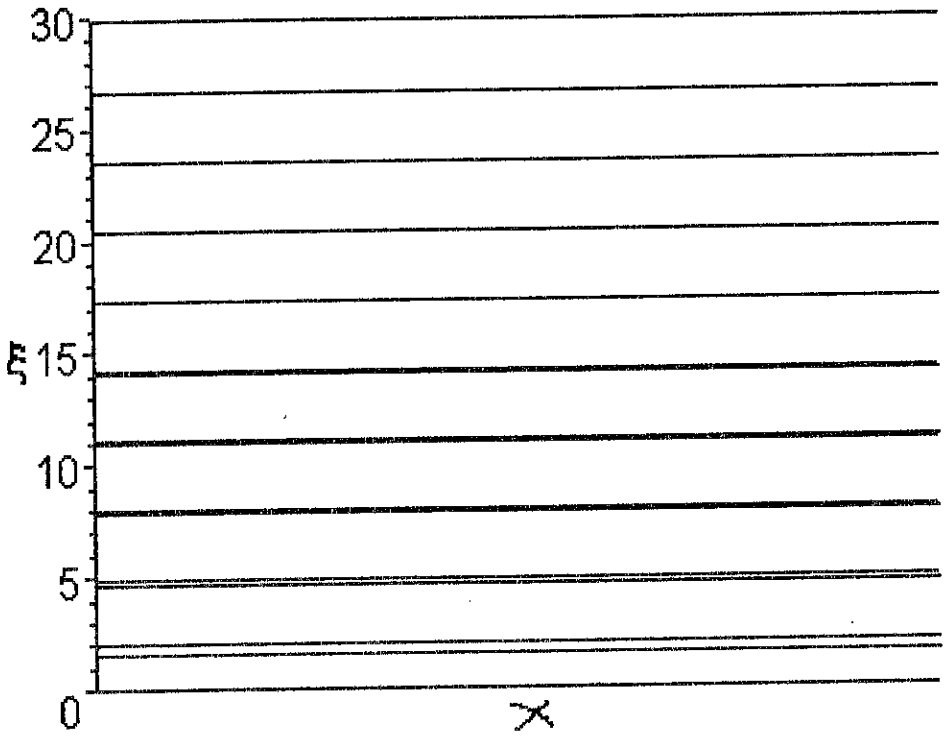

Figure 4.7: Even and odd solutions for the symmetric double well potential when E is close to V_0. The even and odd solutions always appear grouped. The lower lines represent even and the upper ones odd solutions. As ξ increase to be close to V_0, the even and odd solutions degenerate to be the same. Here, V_0 is 30.

4.2 Symmetric Triple Well Potential

We now consider a triple well potential as shown in Figure 4.8. We will again concentrate on finding energy levels below the barrier that is $E \leq V_0$. This one dimensional triple well potential is also symmetric with respect to reflection around its central y-axis. The width of each of the potential well is labeled a, and that of the central barrier is labeled b. We name the regions from left to right, 'Region I,' 'Region II,' 'Region III,' 'Region IV,' and 'Region V,' and establish appropriate eigenfunctions in each region:

for $-3a/2 - b \leq x \leq -a/2 - b$

$$\psi_I(x) = A e^{ikx} + B e^{-ikx}, \tag{4.46}$$

for $-a/2 - b \leq x \leq -a/2$

$$\psi_{II}(x) = C e^{qx} + D e^{-qx}, \tag{4.47}$$

for $-a/2 \leq x \leq a/2$

$$\psi_{III}(x) = F e^{ikx} + G e^{-ikx}, \tag{4.48}$$

for $a/2 \leq x \leq a/2 + b$

$$\psi_{IV}(x) = I e^{qx} + L e^{-qx}, \tag{4.49}$$

and for $a/2 + b \leq x \leq 3a/2 + b$

$$\psi_V(x) = M e^{ikx} + N e^{-ikx}, \tag{4.50}$$

to

$$\cos\left(\frac{3\xi}{2}\right) = -\tanh\left(\sqrt{\lambda^2-\xi^2}\right)\left[\frac{\sqrt{\lambda^2-\xi^2}}{\xi}\sin(\xi)\cos\left(\frac{\xi}{2}\right) - \frac{\xi}{\sqrt{\lambda^2-\xi^2}}\cos(\xi)\sin\left(\frac{\xi}{2}\right)\right] \tag{4.53}$$

$$\sin\left(\frac{3\xi}{2}\right) = -\tanh\left(\sqrt{\lambda^2-\xi^2}\right)\left[\frac{\sqrt{\lambda^2-\xi^2}}{\xi}\sin(\xi)\sin\left(\frac{\xi}{2}\right) + \frac{\xi}{\sqrt{\lambda^2-\xi^2}}\cos(\xi)\cos\left(\frac{\xi}{2}\right)\right] \tag{4.54}$$

for the even and odd solutions, respectively.

The solutions of these equations can be found graphically as the intersections between the curves representing the right-hand side and left-hand side of the equations. Plots can be made to equate the left and the right hand sides of the even and the odd solution equations. Figure 4.9 is such a plot for a particular $\lambda = 12$ value from $E = 0$ to $E = V_0$. Since the horizontal axis represents ξ which is directly related to the energy, this graph simultaneously indicates the position of energy levels within the barrier. Here we can see that two even solutions and one odd solution or one even solution and two odd solutions are grouped, and the order is even-odd-even or odd-even-odd, etc., starting from the lowest energy. In either case we notice the second and third solutions are closer to each other than they are to the first one. We illustrate the global distribution of energy levels below the barrier by plotting ξ as a function of λ, or a measure for the energy as a function of the potential.

We identify the following features: the plot is restricted to values λ and ξ such

that $E < V_0$. The line $\xi = \lambda$ corresponds to the location where levels appear since $E = V_0$. Levels are grouped three by three. The resolution of the plot only allows us to see two dots. An enlargement of the lowest branch in Figure 4.11 shows all three solutions. As λ increases the two (really three) solutions get closer together to merge in the limit $\lambda \to \infty$, the ratio of energy differences between the three components of a triplet is of the order 1/100. In other words, the last two solutions come closer and closer, and finally they become the same value within our finite accuracy and they keep coming closer to the first solution as λ increases more. This means that they degenerate to be one solution when λ is large. This is shown in Figure 4.10 and Figure 4.11. The different spacing between the levels can be understood by the inequivalent nature of the side wells and the central well.

We now derive some results about the general model of the triple well potential. For this model a is different from b. Let $\rho = \frac{b}{a}$, then $b = \rho a$. Then

$$\eta = q b = \rho q a \tag{4.55}$$

and

$$\lambda^2 = \xi^2 + \frac{\eta^2}{\rho^2}. \tag{4.56}$$

With these relations the equations for the even and odd solutions for the triple well potential—(4.51) and (4.52)—can be rewritten as

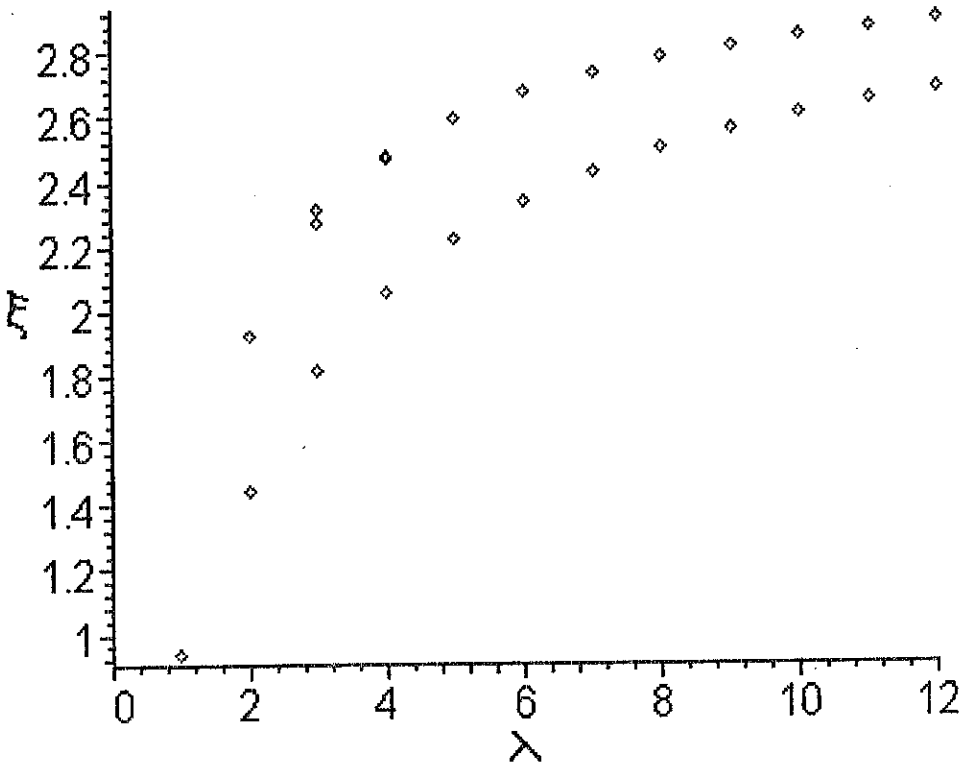

Figure 4.11: ξ vs. λ for the triple well potential. Convergence of the first three solutions of a triple well potential: it is clear that the upper two solutions merge fast into one within our accuracy and finally all three solutions totally coalesce as λ increases.

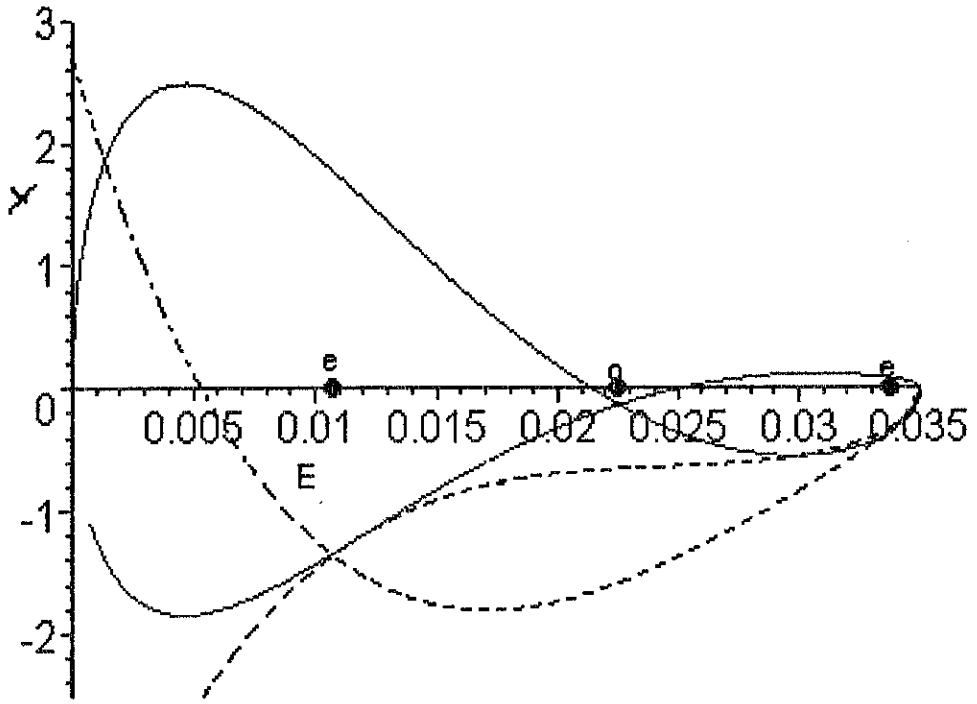

Figure 4.12: The three energy levels for the triple well potential are equally spaced with $\rho = 0.293$. $L = 10\,nm$ and $V_0 = 0.035\,eV$. The intercepts between the dotted lines represent even solutions and that between solid lines represents an odd solution. The dots on the horizontal axis are the reflections of the intersections. The first even solution is 0.01074793099 eV, followed by 0.02254853321 eV (odd) and 0.03434017882 eV (even). The energy difference between the first-middle and the middle-last is 0.895661×10^{-5}.

4.3 Symmetric Quadruple Well Potential

For the quadruple well potential shown in Figure 4.14, I followed similar steps to find the energy solutions. The even and odd solutions are given respectively by

$$2\sqrt{\lambda^2-\xi^2}+\xi[\cot(\xi)-\tan(\xi)]\coth\left(\frac{\sqrt{\lambda^2-\xi^2}}{2}\right)=$$
$$-\tanh\left(\sqrt{\lambda^2-\xi^2}\right)\times$$
$$\left[\frac{\lambda^2-2\xi^2}{\sqrt{\lambda^2-\xi^2}}\coth\left(\frac{\sqrt{\lambda^2-\xi^2}}{2}\right)+\frac{\xi^2\cot(\xi)+(\lambda^2-\xi^2)\tan(\xi)}{\xi}\right] \quad (4.60)$$

$$2\sqrt{\lambda^2-\xi^2}+\xi[\cot(\xi)-\tan(\xi)]\tanh\left(\frac{\sqrt{\lambda^2-\xi^2}}{2}\right)=$$
$$-\tanh\left(\sqrt{\lambda^2-\xi^2}\right)\times$$
$$\left[\frac{\lambda^2-2\xi^2}{\sqrt{\lambda^2-\xi^2}}\tanh\left(\frac{\sqrt{\lambda^2-\xi^2}}{2}\right)+\frac{\xi^2\cot(\xi)+(\lambda^2-\xi^2)\tan(\xi)}{\xi}\right]. \quad (4.61)$$

The energy solutions are shown in Figure 4.15, and the relation between energy and initial potential in Figure 4.16. From the Figure 4.16, we can see that two even and two odd solutions are grouped and as the initial potential barrier increases, the first even and odd solutions get really close, and the other even and odd solutions do the same thing. As the potential barrier is increased, all four solutions will come together.

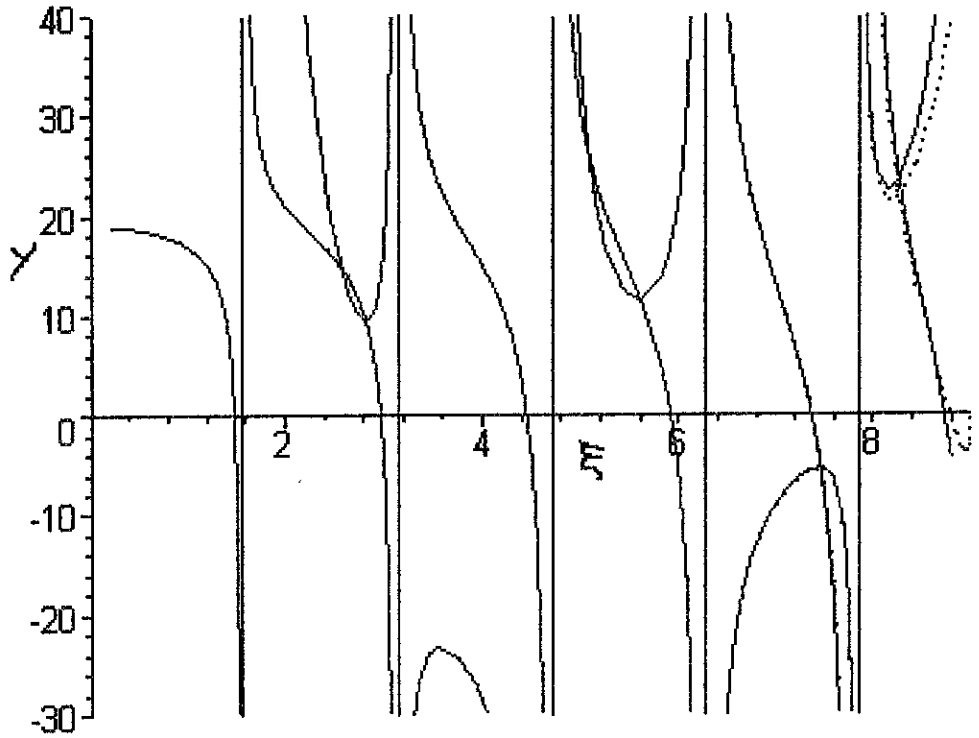

Figure 4.15: Energy Solutions of the Symmetric Quadruple Well Potential. This is the energy solution for the symmetric quadruple well potential when $\lambda = 9$. The solid curves represent even and the dotted curves represent odd solutions. For the lower ξ levels, the even and odd solutions are almost degenerated. The roots are found at 2.563767593, 2.563926478, 2.822588678, 2.822588678; 5.082450444, 5.083324093, 5.610164388, 5.610164391; 7.463209556, 7.471930048, 8.262264948, 8.262281025.

4.4 Symmetric Multi-Well Potential

We now generalize our method to include symmetric multi-well potentials in the special case where $a = b$. Again using symmetry arguments we can consider only the right side of the potential. Starting at the extreme right potential well, we label the constants as A_1, B_1, C_2, D_2, A_3, B_3, C_4, D_4, etc. as shown in Figure 4.17.

The eigenfunctions are the appropriate combinations of sine and cosine function in the wells, whereas they are combinations of hyperbolic sine and hyperbolic cosine functions under the barriers. In the central domain we reserve the letters A and B for classically allowed domains and the letters C and D for classically forbidden domains, we can simply assign sine or cosine when it is a well, or hyperbolic sine or hyperbolic cosine when it is a barrier. Sine and hyperbolic sine correspond to odd solutions whereas cosine and hyperbolic cosine to even solutions.

By applying the boundary conditions starting from the right-most potential wall, we can find the ratios of two constants in each well or barrier. This way of proceeding is similar to the transfer matrix method in multibarrier scattering [8]. Successive ratios can be expressed in terms of previous ratios. For example, the ratio of A_1 and B_1 for a single well potential can be found from the boundary condition at the right-hand wall

$$\frac{A_1}{B_1} = -e^{-ika}. \tag{4.62}$$

$$\frac{A_3}{B_3} = \frac{e^{-3ika}\left[\frac{C_2}{D_2}\left(\frac{ik}{q}+1\right)+e^{-3qa}\left(\frac{ik}{q}-1\right)\right]}{\frac{C_2}{D_2}\left(\frac{ik}{q}-1\right)+e^{-3qa}\left(\frac{ik}{q}+1\right)} \tag{4.68}$$

and for a quintuple well potential

$$\frac{A_1}{B_1} = -e^{-9ika} \tag{4.69}$$

$$\frac{C_2}{D_2} = -\frac{e^{-7qa}\left[\frac{A_1}{B_1}\left(\frac{ik}{q}+1\right)-e^{-7ika}\left(\frac{ik}{q}-1\right)\right]}{\frac{A_1}{B_1}\left(\frac{ik}{q}-1\right)-e^{-7ika}\left(\frac{ik}{q}+1\right)} \tag{4.70}$$

$$\frac{A_3}{B_3} = \frac{e^{-5ika}\left[\frac{C_2}{D_2}\left(\frac{ik}{q}+1\right)+e^{-5qa}\left(\frac{ik}{q}-1\right)\right]}{\frac{C_2}{D_2}\left(\frac{ik}{q}-1\right)+e^{-5qa}\left(\frac{ik}{q}+1\right)} \tag{4.71}$$

$$\frac{C_4}{D_4} = -\frac{e^{-3qa}\left[\frac{A_3}{B_3}\left(\frac{ik}{q}+1\right)-e^{-3ika}\left(\frac{ik}{q}-1\right)\right]}{\frac{A_3}{B_3}\left(\frac{ik}{q}-1\right)-e^{-3ika}\left(\frac{ik}{q}+1\right)} \tag{4.72}$$

and for a sextuple well potential

$$\frac{A_1}{B_1} = -e^{-11ika} \tag{4.73}$$

$$\frac{C_2}{D_2} = -\frac{e^{-9qa}\left[\frac{A_1}{B_1}\left(\frac{ik}{q}+1\right)-e^{-9ika}\left(\frac{ik}{q}-1\right)\right]}{\frac{A_1}{B_1}\left(\frac{ik}{q}-1\right)-e^{-9ika}\left(\frac{ik}{q}+1\right)} \tag{4.74}$$

$$\frac{A_3}{B_3} = \frac{e^{-7ika}\left[\frac{C_2}{D_2}\left(\frac{ik}{q}+1\right)+e^{-7qa}\left(\frac{ik}{q}-1\right)\right]}{\frac{C_2}{D_2}\left(\frac{ik}{q}-1\right)+e^{-7qa}\left(\frac{ik}{q}+1\right)} \tag{4.75}$$

$$\frac{C_4}{D_4} = -\frac{e^{-5qa}\left[\frac{A_3}{B_3}\left(\frac{ik}{q}+1\right)-e^{-5ika}\left(\frac{ik}{q}-1\right)\right]}{\frac{A_3}{B_3}\left(\frac{ik}{q}-1\right)-e^{-5ika}\left(\frac{ik}{q}+1\right)} \tag{4.76}$$

$$\frac{A_5}{B_5} = \frac{e^{-3ika}\left[\frac{C_4}{D_4}\left(\frac{ik}{q}+1\right)-e^{-3qa}\left(\frac{ik}{q}-1\right)\right]}{\frac{C_4}{D_4}\left(\frac{ik}{q}-1\right)+e^{-3qa}\left(\frac{ik}{q}+1\right)} \tag{4.77}$$

where the wavefunction is either $F\cos(kx)$ $(F\sin(kx))$ or $G\cosh(qx)$ $(G\sinh(qx))$

where the constant $a_k = \frac{1}{\sqrt{N}}$ is a normalization factor, and ω_k can be expressed as

$$\omega_k = \omega_0 + \frac{2\pi k}{N\tau} = \omega_0 + \frac{2\pi k}{T}. \tag{4.82}$$

ω_k is the eigenfrequency of the kth state in the triplet starting counting ω_0, and $\hbar\omega_k$ are the energy levels for the stationary states and there is a range in the energy of $\psi(t)$ equal to

$$\epsilon = \hbar(\omega_N - \omega_0) = \frac{2\pi\hbar}{\tau} \tag{4.83}$$

This means that the clock wavefunction $\psi(t)$ cannot move from one well to the other during the time interval T if its energy uncertainty satisfies the relation

$$\epsilon T = N2\pi\hbar \tag{4.84}$$

or the order of the energy uncertainty is

$$\epsilon = \frac{N2\pi\hbar}{T} = \frac{h}{\tau}. \tag{4.85}$$

The well potential has infinity potential at the end walls so a particle confined in the well potential cannot escape from it. As time goes by the clock wave function $\psi(t)$ moves periodically with the period $N\tau = T$ (refer to Page 25). If the spread of energies is too small, then the localization of $\psi(t)$ at different t's is insufficient to claim that the clock ticks every τ. In addition, the energy levels are equally spaced so it does not lead to 'dispersion.' Thus the clock is 'perfect' and is not likely to have dispersion due to the finite number of superposed terms.

Chapter 5

Special Relativity and the Quantum Clock

5.1 Special Relativity and Quantum Clocks

Relativity and quantum mechanics are two of the most successful scientific theories of the twentieth century. Each of them represents a great triumph of the human mind in understanding the universe. Relativity was essentially established Albert Einstein, whereas quantum theory was the product of the work of many scientists around the world. These two realms seemed totally separated, but they were unified by P. A. M. Dirac in 1928 [7]. The Dirac equation in relativistic quantum mechanics exhibits several properties that are typically not associated with the Schrödinger

where $\alpha = \begin{pmatrix} 0 & \vec{\sigma} \\ \vec{\sigma} & 0 \end{pmatrix}$, $\beta = \begin{pmatrix} I & 0 \\ 0 & -I \end{pmatrix}$, m_0 is the rest mass of a Dirac particle, $P(q)$ is a projection operator, and H_c is the Hamiltonian of a clock itself. In addition, $\sigma_x = \begin{pmatrix} 0 & 1 \\ 1 & 0 \end{pmatrix}$, $\sigma_y = \begin{pmatrix} 0 & -i \\ i & 0 \end{pmatrix}$, and $\sigma_z = \begin{pmatrix} 1 & 0 \\ 0 & -1 \end{pmatrix}$ are Pauli spin matrices, I is a unit 2×2 matrix, and $P(q) = 1$ if $0 \leq q \leq L$ and 0 otherwise (q is the position of the clock, and L is the length of the clock) [5]. To measure time with a Dirac particle, we first measure the velocity of the particle within the clock potential from the phase shift which occurs as the particle comes into and goes out of the one dimensional potential barrier whose width is L.

Suppose now that the clock is in one of the energy eigenstates: $\phi = \phi_m$. Then we can obtain an energy eigenvalue equation for ψ:

$$\left(-i\,\alpha \cdot \nabla + \beta\, m_0 + \frac{2\pi\, m\, P(q)}{N\,\tau}\right) \psi = E\,\psi. \tag{5.2}$$

This is the equation of a Dirac particle moving in the square potential $V = V_0 = 2\pi\, m/(N\,\tau)$ for $0 \leq q \leq L$ and $V = 0$ elsewhere. When we consider a clock with an arbitrary spin state, we couple this spin state to the projection operator of the clock as

$$\left(-i\,\alpha \cdot \nabla + \beta\, m_0 + \frac{2\pi\, m\, P(q)\,\sigma \cdot \mathbf{n}}{N\,\tau}\right) \psi = E\,\psi. \tag{5.3}$$

We solve this equation for three regions defined by $q \leq 0$, $0 \leq q \leq L$, and $L \leq q$ by assuming that the plane wave e^{ikq} is initially from left to right, and we can find

time from the velocity which in turn comes from a phase shift occuring in the region $0 \leq q \leq L$.

For the next question relating to the construction of a relativistic clock, I found the solutions of the Dirac equation with single and double square well potentials in analogy with the work for the Schrödinger case in Chapter 4. In this case the relativistic behavior of the clock will be incorporated in the last term of (5.1). One then constructs a superposition of stationary states leading to localized 'clock states.'

5.3 Relativistic Single Square Well Potential

Before solving the Dirac equation in the symmetric one-dimensional rigid double square well potential, we will study a relativistic 'free' particle confined to a one-dimensional infinite square well potential as shown in Figure 5.1 [1, 2, 4]. Let's consider a free electron of mass m_0 moving along the z direction inside the potential. The Dirac equation can be written as

$$H\psi = \left(\alpha_z p_z c + \beta m_0 c^2\right) \psi = E\psi \tag{5.4}$$

where $\alpha_z = \begin{pmatrix} 0 & \sigma_z \\ \sigma_z & 0 \end{pmatrix}$, $\beta = \begin{pmatrix} I & 0 \\ 0 & -I \end{pmatrix}$, and $\sigma_z = \begin{pmatrix} 1 & 0 \\ 0 & -1 \end{pmatrix}$ is a 2×2 Pauli spin matrices, I is a unit 2×2 matrix, and $p_z = -i\hbar\frac{d}{dz}$ is the z component of the momentum operator of the particle.

conditions for the wavefunction and the self-adjointness of the formal Dirac operator [2]. The proper boundary and symmetry conditions with the end walls of the potential well located at $z = 0$ and $z = L$ are

$$\rho(0) = \rho(L) \neq 0 \tag{5.6}$$

$$j_z(0) = j_z(L) = 0 \tag{5.7}$$

where $\rho = \psi^\dagger\psi$ is the Dirac probability density and $j_z = c\psi^\dagger\alpha_z\psi$ is the Dirac probability current. From these boundary conditions and relativistic boundary conditions of the MIT bag model [3] that makes the outward flux of probability at the end walls of the infinite potential well be zero such as

$$\pm(-i)\beta\,\alpha_z\psi = \psi \tag{5.8}$$

where '-' corresponds to the left end wall ($z = 0$) and '+' to the right end wall ($z = L$), we can have a transcendental equation such as [1, 2]

$$\tan(kL) = \frac{2P}{P^2 - 1} = -\frac{\hbar k}{m_0 c} \tag{5.9}$$

where we introduced the following factors:

$$P = \frac{\hbar k c}{E + m_0 c^2} \tag{5.10}$$

$$e^{i\delta} = \frac{iP - 1}{iP + 1} \tag{5.11}$$

$$\delta = \arctan\left(\frac{2P}{P^2 - 1}\right) \tag{5.12}$$

When the length L is equal or smaller than the Compton wavelength of the particle divided by 2π, the particle is considered relativistic and (5.9) can be applied. For example, the Compton wavelength for an electron is about $0.004\mathring{A} = 4.0\times10^{-13}m$. From the discrete values of k which satisfy (5.9), discrete values of energy $E = \sqrt{(\hbar kc)^2 + m_0^2c^4}$ can be obtained. The graphical solution of (5.9) is shown in Figure 5.2. One important remark is that the relativistic energy levels are lower than the corresponding non-relativistic ones [1].

5.4 Relativistic Double Square Well Potential

Now consider a Dirac particle confined to the one-dimensional symmetric double well potential shown in Figure 5.3. We choose z as the relevant coordinate. Therefore, ψ is only a function of z, e.g. $\psi = \psi(z)$. Then the Dirac equations in each domain are following:

$$\left(\alpha_z p_z c + \beta m_0 c^2\right) \psi_I = E\psi_I \tag{5.13}$$

$$\left(\alpha_z p_z c + \beta m_0 c^2\right) \psi_{II} = (E - V_0)\psi_{II} \tag{5.14}$$

$$\left(\alpha_z p_z c + \beta m_0 c^2\right) \psi_{III} = E\psi_{III}. \tag{5.15}$$

Here, $V_0 > m_0c^2 + E$ and $E > m_0c^2$, and if we consider only the 'spin up' case, then the wavefunction solutions to Equations 5.13, 5.14 and 5.15 are respectively

$$\psi_I = Ae^{ip_1z/\hbar}\begin{pmatrix} 1 \\ 0 \\ \frac{p_1c}{E+m_0c^2} \\ 0 \end{pmatrix} + Be^{-ip_1z/\hbar}\begin{pmatrix} 1 \\ 0 \\ \frac{-p_1c}{E+m_0c^2} \\ 0 \end{pmatrix} \tag{5.16}$$

$$\psi_{II} = Ce^{ip_2z/\hbar}\begin{pmatrix} 1 \\ 0 \\ \frac{p_2c}{E+m_0c^2-V_0} \\ 0 \end{pmatrix} + De^{-ip_2z/\hbar}\begin{pmatrix} 1 \\ 0 \\ \frac{-p_2c}{E+m_0c^2-V0} \\ 0 \end{pmatrix} \tag{5.17}$$

$$\psi_{III} = Fe^{ip_1z/\hbar}\begin{pmatrix} 1 \\ 0 \\ \frac{p_1c}{E+m_0c^2} \\ 0 \end{pmatrix} + Ge^{-ip_1z/\hbar}\begin{pmatrix} 1 \\ 0 \\ \frac{-p_1c}{E+m_0c^2} \\ 0 \end{pmatrix} \tag{5.18}$$

where $p_1c = \sqrt{E^2 - m_0^2c^4}$ and $p_2c = \sqrt{(V_0 - E)^2 - m_0^2c^4}$.

As mentioned in Section 5.3 for the single potential well, the symmetry and boundary conditions for the Dirac particle are

$$\rho_I(-a-b/2) = \rho_{III}(a+b/2) \neq 0 \tag{5.19}$$

$$j_{z\,I}(-a-b/2) = j_{z\,III}(a+b/2) = 0 \tag{5.20}$$

$$\begin{pmatrix} 0 & 0 & 1 & 0 \\ 0 & 0 & 0 & -1 \\ 1 & 0 & 0 & 0 \\ 0 & -1 & 0 & 0 \end{pmatrix} \left[Ae^{ip_1 z/\hbar} \begin{pmatrix} 1 \\ 0 \\ \frac{p_1 c}{E+m_0c^2} \\ 0 \end{pmatrix} + Be^{-ip_1 z/\hbar} \begin{pmatrix} 1 \\ 0 \\ \frac{-p_1 c}{E+m_0c^2} \\ 0 \end{pmatrix} \right]$$

$$= \left(AA^* \frac{2p_1c^2}{E+m_0c^2} - BB^* \frac{2p_1c^2}{E+m_0c^2} \right). \tag{5.27}$$

Similarly,

$$j_{z\,II} = \left(CC^* \frac{2p_2c^2}{E+m_0c^2-V_0} - DD^* \frac{2p_2c^2}{E+m_0c^2-V0} \right) \tag{5.28}$$

$$j_{z\,III} = \left(FF^* \frac{2p_1c^2}{E+m_0c^2} - GG^* \frac{2p_1c^2}{E+m_0c^2} \right). \tag{5.29}$$

For the probability density,

$$\rho_I = \psi_I^\dagger \psi_I$$

$$= \left[A^* e^{-ip_1 z/\hbar} \left(1,\ 0,\ \frac{p_1 c}{E+m_0c^2},\ 0 \right) + B^* e^{ip_1 z/\hbar} \left(1,\ 0,\ \frac{-p_1 c}{E+m_0c^2},\ 0 \right) \right] \times$$

$$\left[Ae^{ip_1 z/\hbar} \begin{pmatrix} 1 \\ 0 \\ \frac{p_1 c}{E+m_0c^2} \\ 0 \end{pmatrix} + Be^{-ip_1 z/\hbar} \begin{pmatrix} 1 \\ 0 \\ \frac{-p_1 c}{E+m_0c^2} \\ 0 \end{pmatrix} \right]$$

$$= \left(1 + \frac{p_1^2 c^2}{(E+m_0c^2)^2} \right) (AA^* + BB^*) +$$

and (5.32) as

$$\rho_{III} = \left(1 + \frac{p_1^2 c^2}{(E + m_0 c^2)^2}\right)(AA^* + BB^*) + \left(1 - \frac{p_1^2 c^2}{(E + m_0 c^2)^2}\right)\left(B^* A e^{-2ip_1 z/\hbar} + A^* B e^{2ip_1 z/\hbar}\right). \tag{5.36}$$

The boundary conditions used so far are not sufficient to find the quantized energies. We need something else. According to the MIT bag model [3], the relativistic boundary condition that makes the outward flux of probability at the end walls of the infinite potential well is

$$\pm(-i)\beta\,\alpha_z\psi = \psi \tag{5.37}$$

where '-' corresponds to the left end wall ($z = -a - \frac{b}{2}$) and '+' to the right end wall ($z = a + \frac{b}{2}$). If we multiply (5.37) by $\overline{\psi}$ ($= \psi^\dagger\beta$) from the left, we get

$$\pm(-i)\overline{\psi}\,\beta\,\alpha_z\psi = \pm(-i)\psi^\dagger\beta\,\beta\,\alpha_z\psi \tag{5.38}$$

$$= \pm(-i)\psi^\dagger\alpha_z\psi \tag{5.39}$$

$$= \overline{\psi}\,\psi. \tag{5.40}$$

Note that (5.39) represents the probability current density for a Dirac spinor in the z direction. We can easily check from (5.39) and (5.40) that the outward flux is zero at the end-walls. Thus, (5.37) expresses the same condition as (5.7) at the boundaries $z = -a - \frac{b}{2}$ and $z = a + \frac{b}{2}$.

then

$$B = Ae^{i[\delta - k_1(2a+b)]} \tag{5.46}$$

$$= Ae^{i\Gamma} \tag{5.47}$$

where $\Gamma = \delta - k_1(2a+b)$.

Thus, by using (5.47) $\psi_{III}(z)$ can be rewritten as

$$\psi_{III}(z) = Ae^{i\Gamma}e^{ik_1z}\begin{pmatrix}\chi\\ P_1\chi\end{pmatrix} + Ae^{-ik_1z}\begin{pmatrix}\chi\\ -P_1\chi\end{pmatrix} \tag{5.48}$$

$$= A\begin{pmatrix}(e^{i\Gamma}e^{ik_1z} + e^{-ik_1z})\chi\\ P_1(e^{i\Gamma}e^{ik_1z} - e^{-ik_1z})\chi\end{pmatrix} \tag{5.49}$$

$$= Ae^{i\Gamma/2}\begin{pmatrix}2\cos(k_1z + \frac{\Gamma}{2})\chi\\ 2iP_1\sin(k_1z + \frac{\Gamma}{2})\chi\end{pmatrix} \tag{5.50}$$

Since

$$\psi_{II}(z) = Ce^{ik_2z}\begin{pmatrix}\chi\\ P_2\chi\end{pmatrix} + De^{-ik_2z}\begin{pmatrix}\chi\\ -P_2\chi\end{pmatrix}, \tag{5.51}$$

from (5.26) we can finally find two equations for the solutions such as

$$Ce^{ik_2b/2} + De^{-ik_2b/2} = 2Ae^{i\Gamma/2}\cos\left(\frac{k_1b}{2} + \frac{\Gamma}{2}\right) \tag{5.52}$$

$$CP_2e^{ik_2b/2} - DP_2e^{-ik_2b/2} = 2iAP_1e^{i\Gamma/2}\sin\left(\frac{k_1b}{2} + \frac{\Gamma}{2}\right). \tag{5.53}$$

$$= C \begin{pmatrix} 2i\sin(k_2 z)\chi \\ 2P_2\cos(k_2 z)\chi \end{pmatrix}. \tag{5.61}$$

Therefore, when $C = D$, (5.52) and (5.53) can be rewritten as

$$2C\cos\left(\frac{k_2 b}{2}\right) = 2Ae^{i\Gamma/2}\cos\left(\frac{k_1 b}{2}+\frac{\Gamma}{2}\right) \tag{5.62}$$

$$2iCP_2\sin\left(\frac{k_2 b}{2}\right) = 2iAP_1 e^{i\Gamma/2}\sin\left(\frac{k_1 b}{2}+\frac{\Gamma}{2}\right), \tag{5.63}$$

and the two homogeneous equations of (5.62) and (5.63) are

$$C\cos\left(\frac{k_2 b}{2}\right) - Ae^{i\Gamma/2}\cos\left(\frac{k_1 b}{2}+\frac{\Gamma}{2}\right) = 0 \tag{5.64}$$

$$CP_2\sin\left(\frac{k_2 b}{2}\right) - AP_1 e^{i\Gamma/2}\sin\left(\frac{k_1 b}{2}+\frac{\Gamma}{2}\right) = 0. \tag{5.65}$$

Since there exist solutions when the determinant of (5.64) and (5.65) are zero, we have

$$\begin{vmatrix} \cos(\frac{k_2 b}{2}) & -e^{i\Gamma/2}\cos(\frac{k_1 b}{2}+\frac{\Gamma}{2}) \\ P_2\sin(\frac{k_2 b}{2}) & -P_1 e^{i\Gamma/2}\sin(\frac{k_1 b}{2}+\frac{\Gamma}{2}) \end{vmatrix} = 0. \tag{5.66}$$

Thus, from (5.66) we have

$$\tan\left(\frac{k_2 b}{2}\right) = \frac{P_1}{P_2}\tan\left(\frac{k_1 b}{2}+\frac{\Gamma}{2}\right). \tag{5.67}$$

For the special case that $a = b$, (5.67) can be rewritten as

$$\tan\left(\frac{\eta}{2}\right) = \frac{E+m_0c^2-V_0}{E+m_0c^2}\tan\left(\frac{k_1 a}{2}+\frac{\delta-2k_1 a-k_1 a}{2}\right) \tag{5.68}$$

$$\tan\left(\frac{1}{2}\arctan\left(-\frac{\sqrt{\Omega^2-\frac{m_0^2c^4}{V_0^2}}}{\frac{m_0c^2}{V_0}}\right)-\frac{aV_0\sqrt{\Omega^2-\frac{m_0^2c^4}{V_0^2}}}{\hbar c}\right) \tag{5.75}$$

$$\cot\left(\frac{aV_0\sqrt{(1-\Omega)^2-\frac{m_0^2c^4}{V_0^2}}}{2\hbar c}\right)=-\left(1-\frac{1}{\Omega+\frac{m_0c^2}{V_0}}\right)\times$$

$$\tan\left(\frac{1}{2}\arctan\left(-\frac{\sqrt{\Omega^2-\frac{m_0^2c^4}{V_0^2}}}{\frac{m_0c^2}{V_0}}\right)-\frac{aV_0\sqrt{\Omega^2-\frac{m_0^2c^4}{V_0^2}}}{\hbar c}\right). \tag{5.76}$$

Therefore, (5.75) and (5.76) are the final solutions for the relativistic symmetric double well potential. By plotting them for Ω, we can find the energy solutions from the relation $\Omega=\frac{E}{V_0}$. For example, when $a=0.004\mathring{A}=4.0\times10^{-13}m$, $m_0c^2=0.5MeV$, $V_0=10\times m_0c^2$, and $\hbar c=197eV\cdot nm$ ($E>m_0c^2$ and $|V_0-E|>m_0c^2$), the plots are shown in Figure 5.4 and 5.5.

The terms 'even' and 'odd' which were used in the Schrödinger case do not apply here in the same way. (5.75) applies to the case $C=D$ corresponding to an even first component of the spinor and an odd third component.

In conclusion, we have found the transcendental equation giving the energy levels of a particle in a double well. The equations were obtained by combining the boundary conditions at all intermediate boundaries which can be expressed either in terms of the continuity of all components of ψ or as the continuity of both ρ and j. Indeed, the different components of the spinor behave differently under parity.

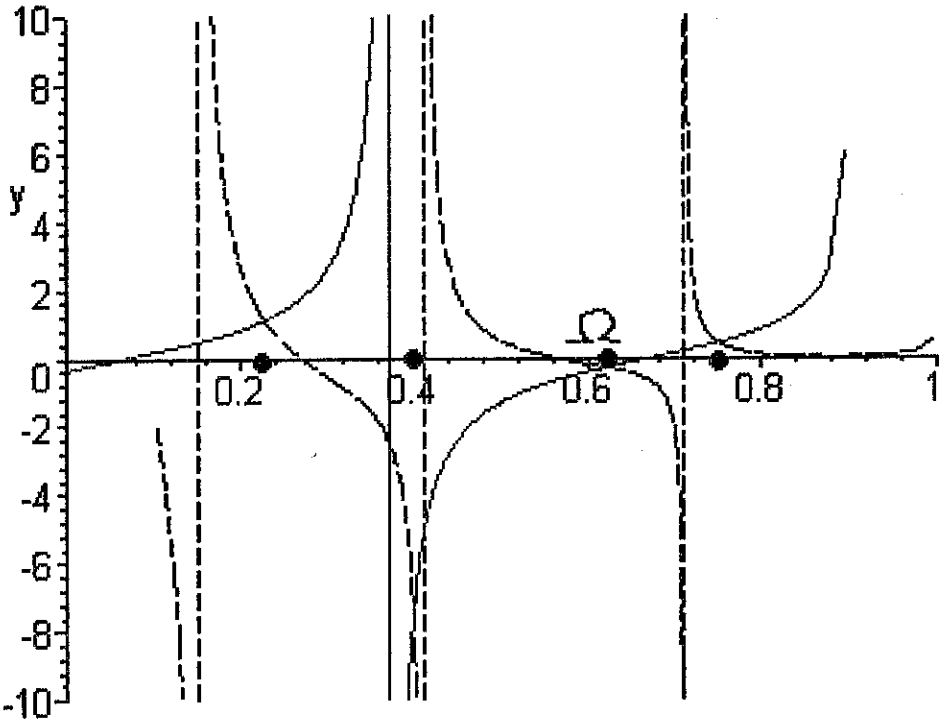

Figure 5.5: The plot of (5.76) when $a = 0.004\mathring{A} = 4.0 \times 10^{-13}m$, $V_0 = 5MeV$. The solid curve is for the left-hand side of the equation and the dotted line for the right-hand side of the equation. The intersections are the values of Ω which are projected on the horizontal axis (big dots). They are from the smallest one 0.2288416918, 0.3988894183, 0.6212410231 and 0.7487633999.

Chapter 6

Conclusion

My study of quantum clocks confirms the realizability of Salecker and Wigner's clock and shows the possibility of constructing a simple one-dimensional model of a clock. In addition, it shows that the dispersion can be removed with sufficient accuracy by making the spacing between energy levels equal. Then, the clock can run accurately for an arbitrary amount of time. This can be done by adjusting the ratio between the widths of the well and barrier in the Schrödinger case.

We can probably argue the same thing for the relativistic quantum clock. For the relativistic case the boundary condition is different from that for the Schrödinger case. For this case the wavefunction is not zero at the wall of the infinite potential well. Because the wavefunction is a spinor of four complex components and it is coupled in a system of first-order differential equations, the requirement that the

far my analysis has been limited to the clock itself. I assumed that the clock was not interacting with anything else; it was just running. For the clock to be useful in a practical sense, a measurement has to happen. At the quantum level a measurement is described by the interaction between the system and the measuring apparatus. Eventually, the measurement will have to be recorded by a macroscopic device as pointed out by von Neumann [16]. Our carefully crafted clock will have to interact with its surroundings and other physical systems. In the process, energy will be exchanged and the system and clock will affect each other. The quantum limitations still apply.

Finally, we should mention that both our notion of the concept of time and our understanding of the structure of quantum mechanics may very well change in the future. The intense efforts presently underway to understand both the ultimate building blocks of matter and the large-scale structure of the universe are leading towards a need for the unification of general relativity and quantum theory. In that process both theories are likely to change and with them so will our understanding of the concept of time and that of quantization. The quantum clock of the future may be very different from that of today.

Still, it gives satisfaction to discover that physical systems at the microscopic level can presently mimic time: there is room for cautiously measuring time in quan-

Bibliography

[1] P. Alberto et al., Eur. J. Phys. **17**, 19 (1996).

[2] V. Alonso et al., Eur. J. Phys. **18**, 315 (1997).

[3] A. Chodos et al., Phys. Rev. D **9**, 3471 (1974).

[4] B. L. Coulter and C. G. Adler, Am. J. Phys. **39**, 305 (1971).

[5] P. C. W. Davis, J. Phys. A **19**, 2115 (1986).

[6] P. C. W. Davis, *About Time*, (New York: Simon & Schuster, 1995).

[7] P. A. M. Dirac, Roy. Soc. Proc., A **117**, 610 (1928).

[8] G. R. Fowles, *Introduction to Modern Optics*, (New York: Holt, Rinehart and Winston, 1975).

[9] W. Greiner, *Relativistic Quantum Mechanics*, (New York: Springer-Verlag, 1994).

[21] G. J. Whitrow, *What is Time*, (London: Thames and Hudson, 1972).

[22] G. J. Whitrow, *The Natural Philosophy of Time*, (Oxford: Oxford University Press, 1980).

[23] H. D. Zeh, *The Direction of Time*, (New York: Spring-Verlag, 1989).

theory is based on the discreteness and randomness of microscopic physical processes. It really provides a new set of physical rules and a new view of the measurement process. The Schrödinger equation in quantum theory replaces Newton's second law. Both theories contain time in the differential equation as a mathematical parameter; however, the Schrödinger equation is first order in time, whereas Newton's second law is second order.

In quantum mechanics all physical observables can be represented by mathematical operators. For example, the energy of a quantum system is represented by the Hamiltonian operator, a position of a particle by a position operator, and a momentum of a particle by a momentum operator. Time, however, remains as a parameter in the quantum mechanical equation, not being transformed into an operator [18]. Then, how can we measure time in quantum mechanics?

1.3 Time in This Work

In this thesis I add my modest contribution to the problem of how to measure time. In Chapter 2 I will describe the general background and definition of a quantum clock, and two models of a quantum clock—Salecker and Wigner's model and Peres's model—will be introduced. In Chapter 3 the Hamiltonian of the quantum clock will be discussed, and it will be shown how the quantum clock wavefunction evolves as

The quantum clock is a dynamical quantum system which in constant time intervals passes through its successive states, and tells coordinate time by measuring the beginning and end of the time interval. A clock-time operator discriminates between the clock's specific time readings. When coupled to another physical system, it can measure the duration of a physical process and keep a permanent record of it. It can even control the duration of a physical process. This is done by combining the time-independent Hamiltonian of the system, the clock, and the interaction between the two.

However, there is a limitation for a quantum clock to serve its purpose. A clock, for instance, is interacting with an apparatus. In order to know what time it is, we have to read on the clock the value of an observable Q which is an angular position of a clock pointer, and the observable should satisfy the following relation [17]

$$\frac{d\langle Q\rangle}{dt} = \frac{i}{\hbar}\left\langle [\hat{H}, Q]\right\rangle \tag{2.1}$$

and therefore

$$\Delta E\,\Delta Q \geq \frac{\hbar}{2}\left|\frac{d\langle Q\rangle}{dt}\right|. \tag{2.2}$$

In order that the clock functions, the expectation value $\langle Q\rangle$ must depend on time and this change in $\langle Q\rangle$ must be greater than the standard deviation ΔQ to be significant. If the clock is observed for a time t through which the clock interacts with the

measurement because the use of macroscopic objects such as a measuring rod would affect the measurement. The accuracy of the running time of the quantum clock is related to the minimum uncertainty of the clock mass. They found that the time resolution was inversely proportional to the energy exchange between the clock and the system with which it interacted. Thus, the clock modified the evolution of the system it measured.

Salecker and Wigner mainly tried to answer the question about the minimum mass and mass (or energy) uncertainty of the clock, but I will not tackle this problem in my thesis. Instead, I will check if there is a dispersion arising from this model and try to get the verification of constructing and functioning of this kind of clock by removing the dispersion.

2.3 Peres's Quantum Clock

In 1980 A. Peres constructed explicitly a time-independent Hamiltonian for the quantum clock and described three possible uses of the clock: velocity determination by a time-of-flight measurement, study of the decay time of an unstable system, and the control of precession of spin in a magnetic field which is turned on and off at prescribed times [18]. He was mainly concerned with how much a system was perturbed by its coupling to a physical clock and how the clock could keep a permanent

where $m = -j, ..., j,\ 0 \leq \theta \leq 2\pi$, and j is an integer number. Then an alternative orthogonal basis ϕ for the wave function is given by

$$\begin{aligned} \phi_k(\theta) &= \frac{1}{\sqrt{N}} \sum_m e^{2\pi i k m/N} \psi_m \\ &= \frac{1}{\sqrt{2\pi N}} \frac{\sin[\frac{N}{2}(\theta - \frac{2\pi k}{N})]}{\sin[\frac{1}{2}(\theta - \frac{2\pi k}{N})]} \end{aligned} \tag{3.2}$$

where $k = 0, ..., N-1$, and $N = 2j+1$, corresponding to sharp peaks for large N at $\theta = \frac{2\pi k}{N}$, with an angular uncertainty $\pm \frac{\pi}{N}$. These sharp peaks indicate that the quantum clock points to the hours labeled by "k." Some examples of the sharp peaks are in Figure 3.1 and 3.2.

3.2 The Time Operator of the Quantum Clock

The operator of the quantum clock time is

$$T_c = \tau \sum m P_m \tag{3.3}$$

where τ is a time resolution or an accuracy of the quantum clock, and P_m is the projection operator of the quantum clock. If we apply the operator to the states of the quantum clock, then

$$P_m \phi_k = \delta_{mk} \phi_k. \tag{3.4}$$

The time of the quantum clock is given by

$$T_c \phi_k = t_k \phi_k \tag{3.5}$$

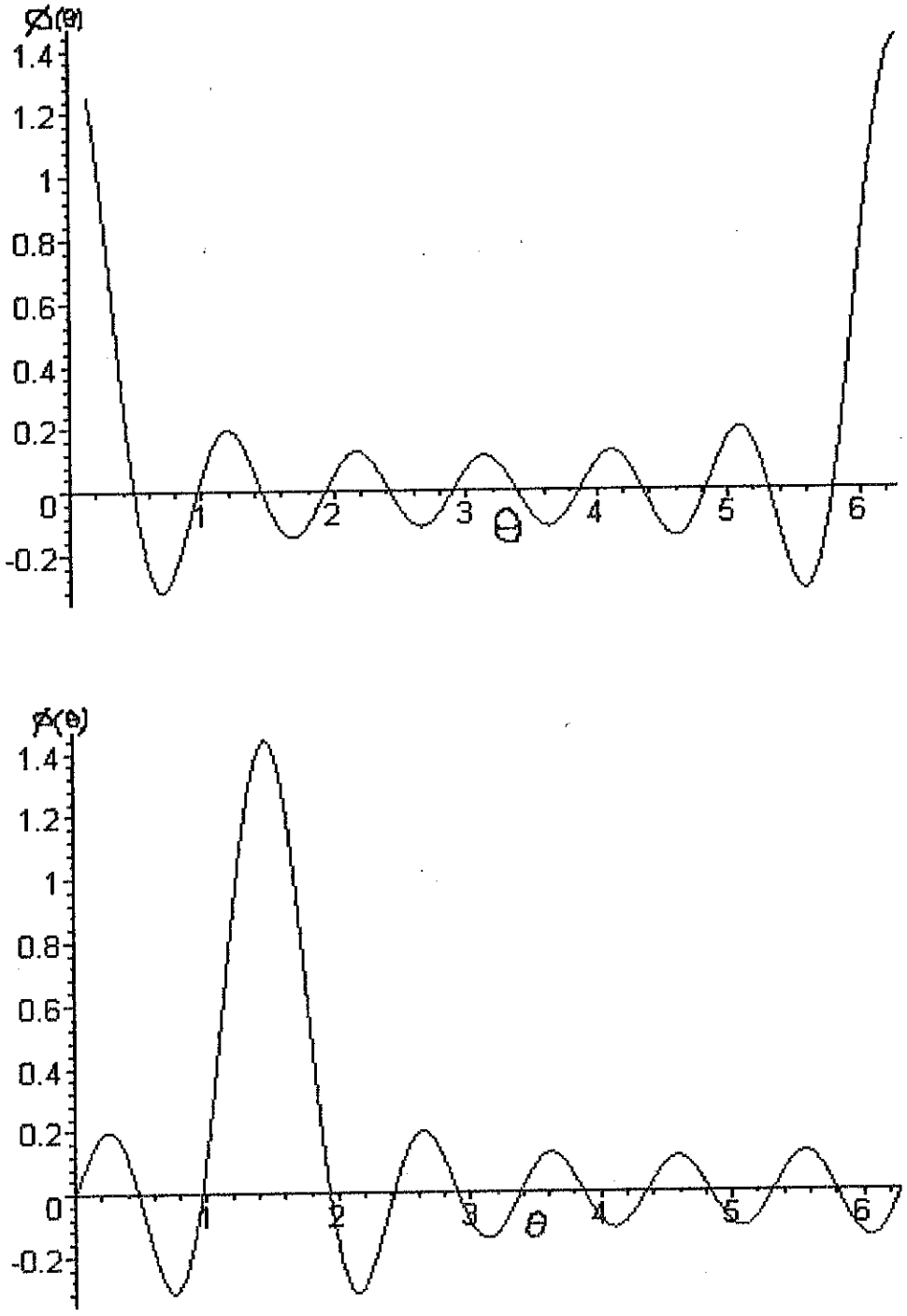

Figure 3.1: The sharp peaks of $\phi_k(\theta)$ occurring in Peres's quantum clock. $N = 13$, $k = 0$ (top) and $k = 3$ (bottom).

indicating that the quantum clock passes successively through the states ϕ_0, ϕ_1, $\phi_2, \ldots$ at time interval τ, and a measure for its energy uncertainty is

$$E = \hbar(\omega - \omega_0) = 2\pi\hbar/\tau \tag{3.10}$$

where $\omega = \omega_0 + 2\pi k/(N\tau)$.

The total Hamiltonian of the system is

$$\begin{aligned} H &= H_p + P(q)\, H_c \\ &= H_p(q,p) + P(q)\, \omega J, \end{aligned} \tag{3.11}$$

where H_p is the Hamiltonian for the dynamical system and $P(q)$ is a projection operator which is 1 when the clock is on, and 0 when off. The second term leads to a potential barrier for the dynamical system described by H_p.

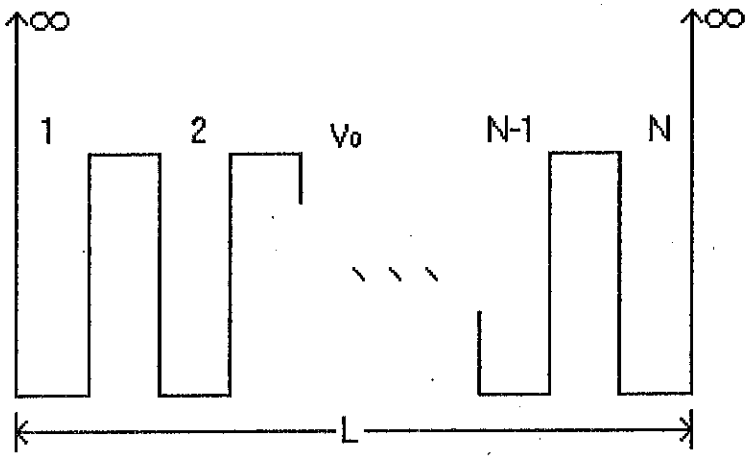

Figure 4.1: N periodic well potential: a potential with N narrow wells and $N-1$ narrow barriers confines a particle and has clusters of N very closely spaced energy levels. The N grouped wave functions are superposed and move, in a time τ, from one well to the other. They, therefore, indicate a specific time. This kind of potential is a good example of the quantum clock of very small size.

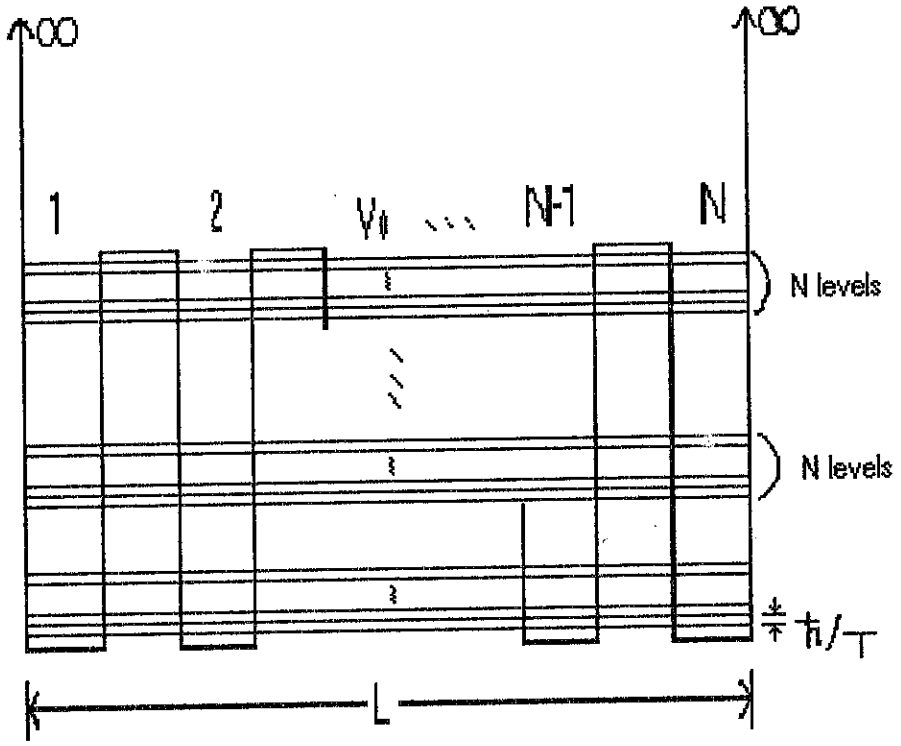

Figure 4.2: Energy levels of N periodic well potential. This kind of potential has a lot of very closely spaced energy levels clustered in groups of N. The energy level spacing is $\frac{\hbar}{T}$.

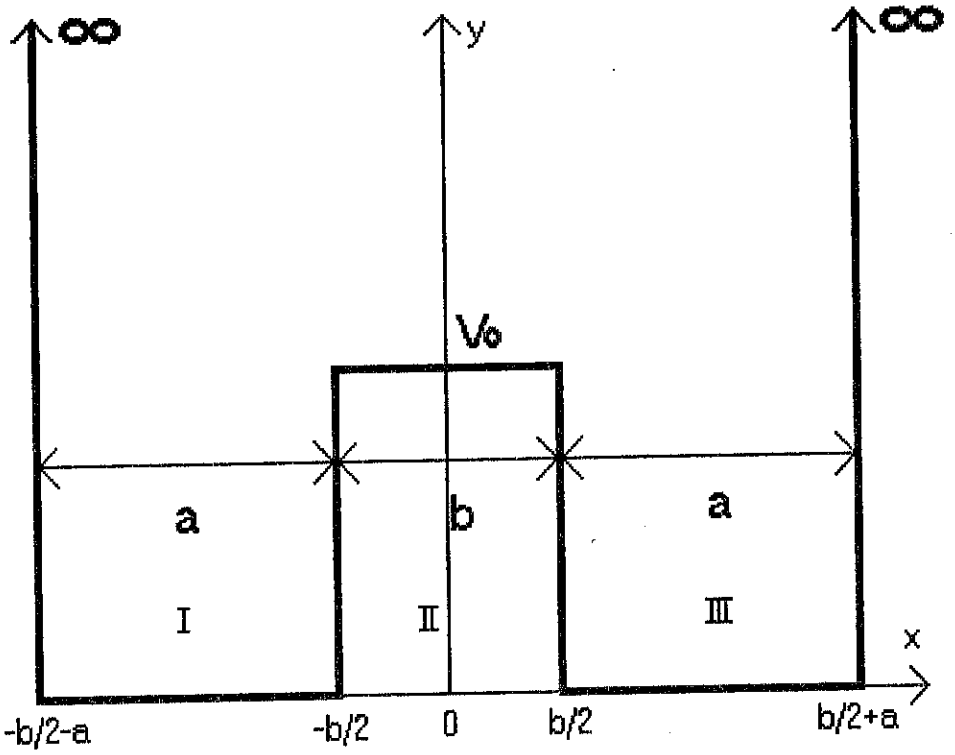

Figure 4.3: This one dimensional double well potential is symmetric with respect to its central y-axis. The width of each of the potential well is a and that of the central barrier is b. The potential energy is V_0 at the top of the barrier. Three regions are distinguished, from left to right, 'Region I,' 'Region II,' and 'Region III.'

which is

$$|\psi(x)| = |\psi(-x)|\,. \tag{4.12}$$

Therefore,

$$\begin{aligned} \psi(x) &= e^{i\alpha}\psi(-x) \\ &= e^{i\alpha}\, e^{i\alpha}\psi(-(-x)) \\ &= e^{2i\alpha}\psi(x) \end{aligned} \tag{4.13}$$

where the phase α is some real constant. Thus,

$$e^{2i\alpha} = 1 \tag{4.14}$$

$$\cos(2\,\alpha) + i\,\sin(2\,\alpha) = 1. \tag{4.15}$$

So

$$\alpha = n\pi \tag{4.16}$$

where $n = 0,\ 1,\ 2,\ 3, \ldots$.

Therefore, there are only two possible choices: $e^{i\alpha} = +1$ (positive parity or symmetric solution) or $e^{i\alpha} = -1$ (negative parity or antisymmetric solution), and the possible forms for the wave function are

$$\psi_I(-x) = \pm\,\psi_{III}(x). \tag{4.17}$$

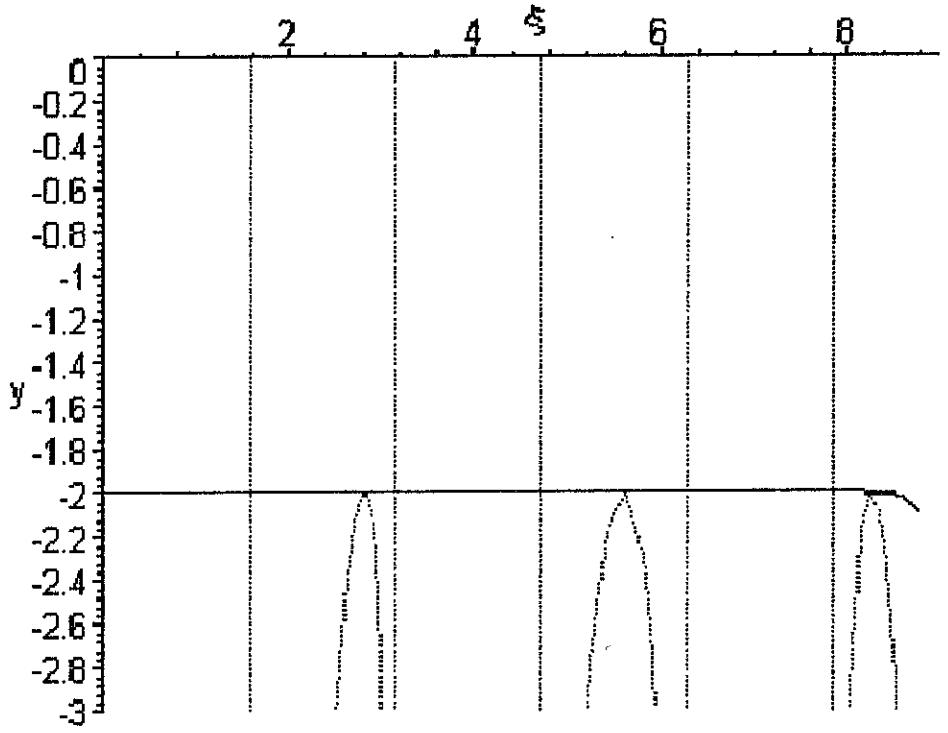

Figure 4.4: Even and odd solutions for the symmetric double well potential with $\lambda = 9$. The straight line represents $-2\coth\left(\sqrt{\lambda^2-\xi^2}\right)$ and the parabolas $\frac{\sqrt{\lambda^2-\xi^2}}{\xi}\tan(\xi) + \frac{\xi}{\sqrt{\lambda^2-\xi^2}}\cot(\xi)$. There are two solutions at the top of each parabola. The two solutions are very close each other and are almost degenerate as λ increases. The roots are found at 2.822485029, 2.822692268, 5.609414347, 5.610913783, 8.246498167, and 8.278652604.

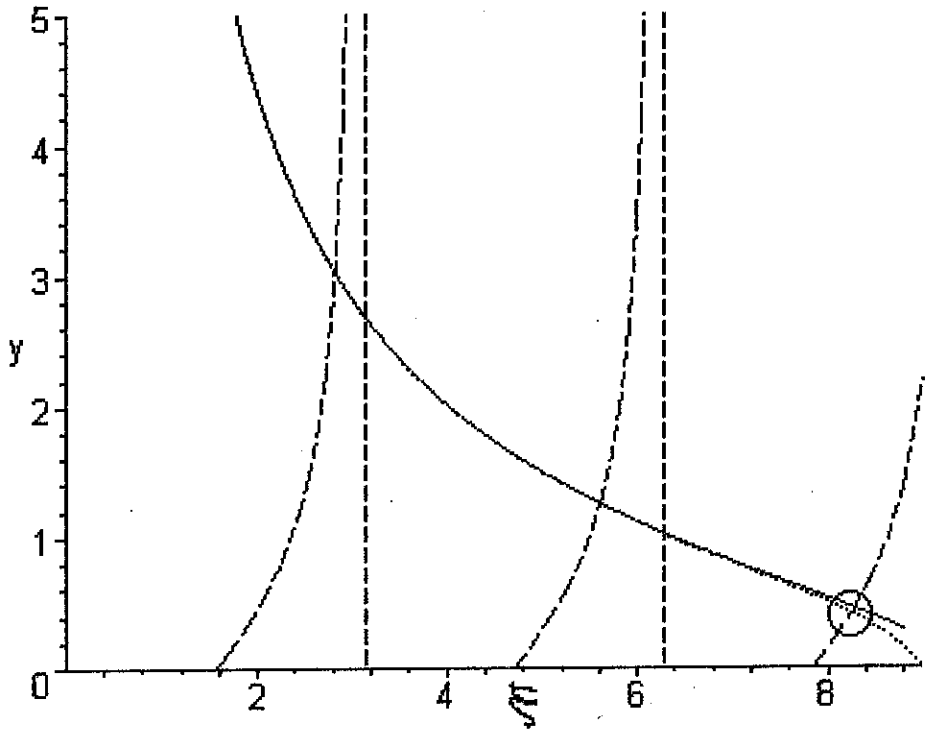

Figure 4.5: Even and odd solutions for the symmetric double well potential with $\lambda = 9$. The long-dotted curves are for $-\cot(\xi)$. The vertical long-dotted lines are asymptotic lines. The intercepts of the long-dotted curves with the short-dotted lines represent even solutions and with the solid line odd solutions. Note that the even and odd solutions have almost the same values except the very upper level solutions (inside the circle) since the solid line and the short-dotted line are almost identical. The roots are found at 2.822485029, 2.822692268, 5.609414347, 5.610913783, 8.246498167, and 8.278652604.

barrier. Note that the value of ξ of each couple of even and odd solutions is lower than that of $\xi(= n\pi, n = 1, 2, 3, \ldots)$ in a single infinite well potential.

If the central barrier potential V_0 goes to infinity, so does λ, and the equations above become

$$-\cot(\xi) = \lim_{\lambda\to\infty} \frac{\sqrt{\lambda^2 - \xi^2}}{\xi} \tanh\left(\frac{\sqrt{\lambda^2 - \xi^2}}{2}\right) = \infty \tag{4.35}$$

$$-\cot(\xi) = \lim_{\lambda\to\infty} \frac{\sqrt{\lambda^2 - \xi^2}}{\xi} \coth\left(\frac{\sqrt{\lambda^2 - \xi^2}}{2}\right) = \infty \tag{4.36}$$

and the solution in both cases is

$$\sin(\xi) = 0 \tag{4.37}$$

which is

$$\xi = n\pi. \tag{4.38}$$

Since $\xi = ka$ and $k = \frac{\sqrt{2mE}}{\hbar}$,

$$E = n^2 \frac{\pi^2\hbar^2}{2ma^2} \tag{4.39}$$

where $n = 1, 2, 3, \ldots$, and these are the energy states for a single infinite well potential. We have recovered the solution of the single well, indicating no coupling between the two wells.

We now look for energy levels at the potential barrier, E is close to V_0, which corresponds to ξ close to λ. Then the solution reduces in the even case to

$$\cos(\xi) = 0. \tag{4.40}$$

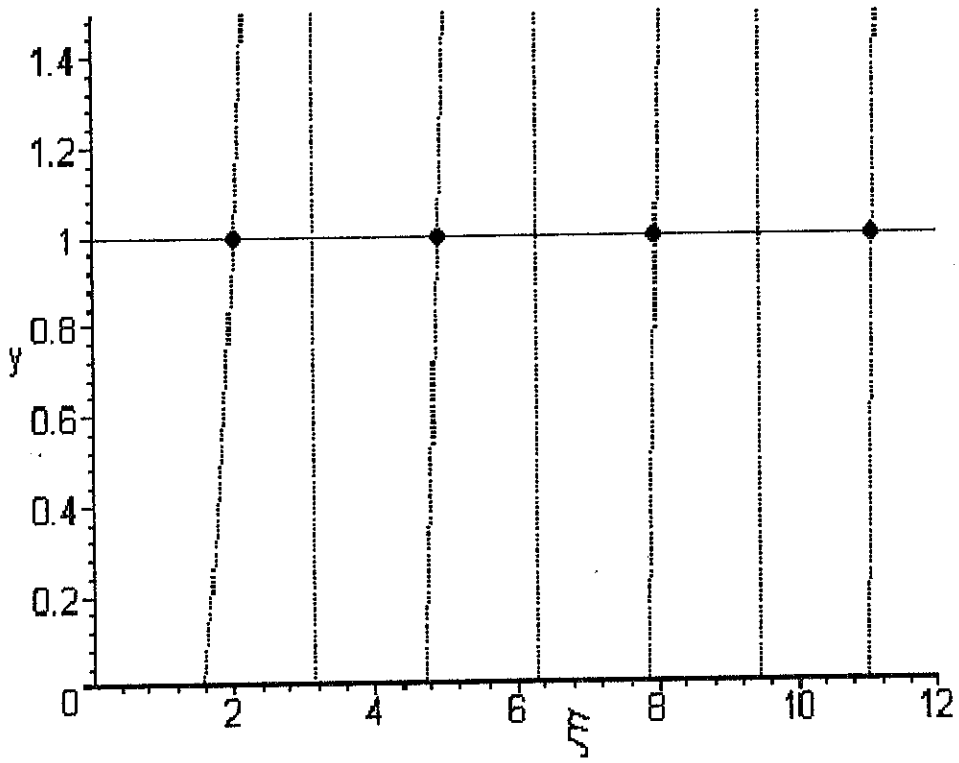

Figure 4.6: Odd energy solutions for the symmetric double well potential when E is close to V_0. The dotted lines are for $-\xi\cot(\xi)$ and the solid line is for 1. The dots on the horizontal solid line represent the intersections between $y = -\xi\cot(\xi)$ and $y = 1$. The roots are found at 2.028757838, 4.913180439, 7.978665712, and 11.08553841.

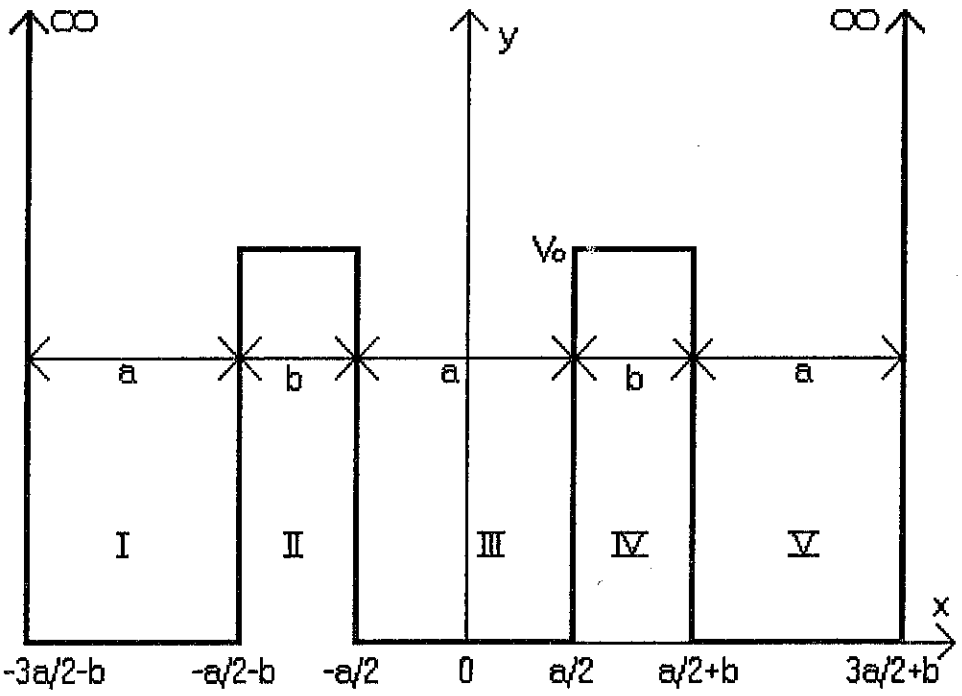

Figure 4.8: This one dimensional triple well potential is symmetric with respect to its central y-axis. The width of each of the potential wells is a and that of the central barriers is b. The potential energy is V_0 at the top of the barrier. Five regions are distinguished, from left to right, 'Region I,' 'Region II,' 'Region III,' 'Region IV,' and 'Region V.'

where A, B, C, D, F, G, I, L, M and N are constants to be determined and k and q are again defined as $k = \frac{\sqrt{2mE}}{\hbar}$, and $q = \frac{\sqrt{2m(V_0-E)}}{\hbar}$.

By analogy with our discussion in Section 4.1, we can show that the symmetry $(x \longrightarrow -x)$ imposes the following simultaneous relations $A = \pm N$, $B = \pm M$, $C = \pm L$ and $D = \pm I$ where the upper (lower) sign refers to the even (odd) solution. Inside the central potential well, the eigenfunction is $Q\cos(kx)$ $(Q\sin(kx))$, where Q is a constant given by $Q = F+G$ $(Q = i(F-G))$ for even (odd) solutions. This symmetric treatment reduces the ten constants to five, and we can consider only the right-half of the figure to find energy solutions. We apply the boundary conditions by imposing continuity in the wavefunction and continuity of its derivative at $x = a/2,\ a/2 + b$ and by imposing continuity in the wavefunction at $3a/2 + b$. By doing this we can construct a 5×5 matrix equation, and solving the determinant of the matrix yields one transcendental equation for the even and the odd solutions:

even:

$$\cos\left(\frac{3ka}{2}\right) = -\tanh(qb)\left[\frac{q}{k}\sin(ka)\cos\left(\frac{ka}{2}\right) - \frac{k}{q}\cos(ka)\sin\left(\frac{ka}{2}\right)\right] \qquad (4.51)$$

odd:

$$\sin\left(\frac{3ka}{2}\right) = -\tanh(qb)\left[\frac{q}{k}\sin(ka)\sin\left(\frac{ka}{2}\right) + \frac{k}{q}\cos(ka)\cos\left(\frac{ka}{2}\right)\right]. \qquad (4.52)$$

When $a = b$, by using λ and ξ defined in Section 4.1, (4.51) and (4.52) simplify

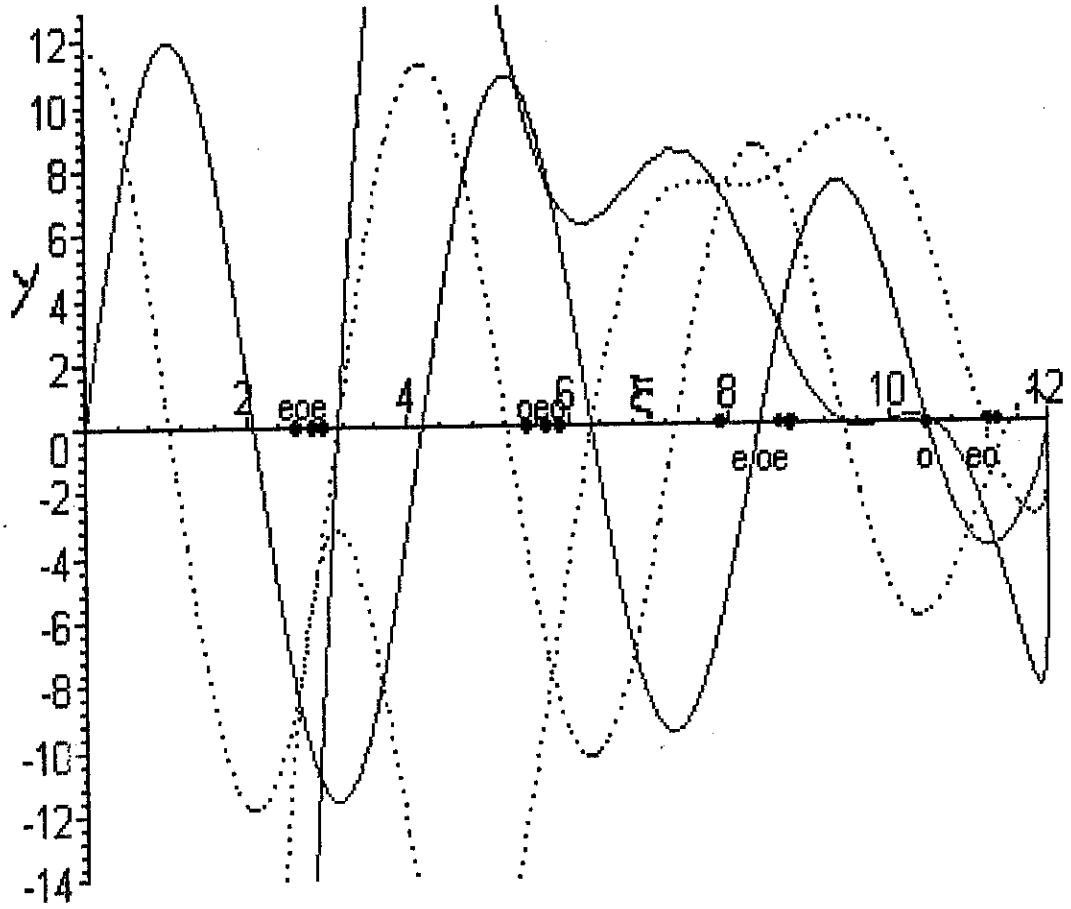

Figure 4.9: Even and odd solutions for the symmetric triple well potential with $\lambda = 12$. The intersections of the dotted lines represent even solutions and the intersections between the solid lines represent odd solutions. The dots on the horizontal axis are the reflections of the intersections. Note that every three solutions appear grouped. The roots are found at 2.689502091, 2.897706546, 2.897706547; 5.357566216, 5.780575082, 5.780575084; 7.971652381, 8.623013258, 8.623013398; 10.45192739, 11.33111190, 11.33135433.

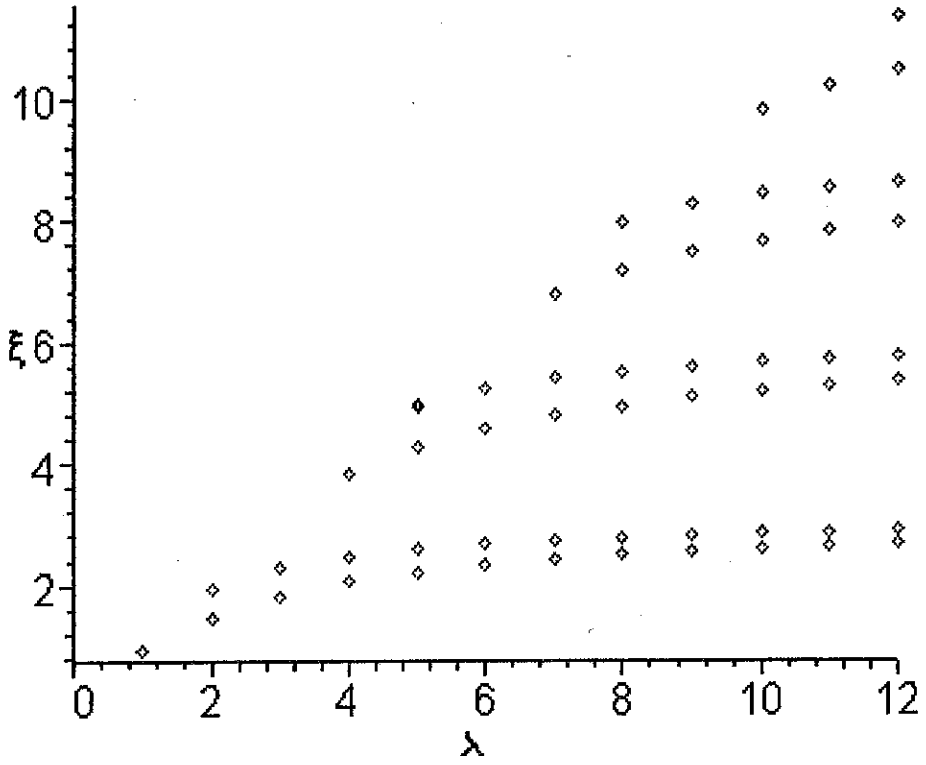

Figure 4.10: ξ vs. λ for the triple well potential. This is the corresponding ξ (related to E) values for integer values of λ (related to V_0). The resolution makes it hard to differentiate two solutions grouped in the upper dots. As λ increases the two (really three) solutions get closer together to merge in the limit $\lambda \to \infty$, the ratio of energy differences between the three components of a triplet is of the order 1/100.

even:

$$\cos\left(\frac{3\xi}{2}\right) = -\tanh\left(\rho\sqrt{\lambda^2-\xi^2}\right)\left[\frac{\sqrt{\lambda^2-\xi^2}}{\xi}\sin(\xi)\cos\left(\frac{\xi}{2}\right) - \frac{\xi}{\sqrt{\lambda^2-\xi^2}}\cos(\xi)\sin\left(\frac{\xi}{2}\right)\right] \tag{4.57}$$

odd:

$$\sin\left(\frac{3\xi}{2}\right) = -\tanh\left(\rho\sqrt{\lambda^2-\xi^2}\right)\left[\frac{\sqrt{\lambda^2-\xi^2}}{\xi}\sin(\xi)\sin\left(\frac{\xi}{2}\right) + \frac{\xi}{\sqrt{\lambda^2-\xi^2}}\cos(\xi)\cos\left(\frac{\xi}{2}\right)\right] \tag{4.58}$$

By adjusting the magnitude of ρ, we can change the relative spacing of the three levels in the triplet. In particular we can space them equally in one of the triplets. However, not all grouped solutions are equally spaced simultaneously for a specific value of ρ. In order for this triple well potential to be applied for the Salecker-Wigner model of the quantum clock, we need to pick up one group of three equally spaced triplets.

To illustrate this in the microworld, we fix the length of the triple potential to be $L = 10\,nm$. Then the width of the well a is

$$a = \frac{L}{3+2\rho} = \frac{10nm}{3+2\rho}. \tag{4.59}$$

When $V_0 = 0.035\,eV$, there are only three solutions and choosing $\rho = 0.293$ the three solutions are equally spaced within our accuracy as shown in Figure 4.12 and Figure 4.13.

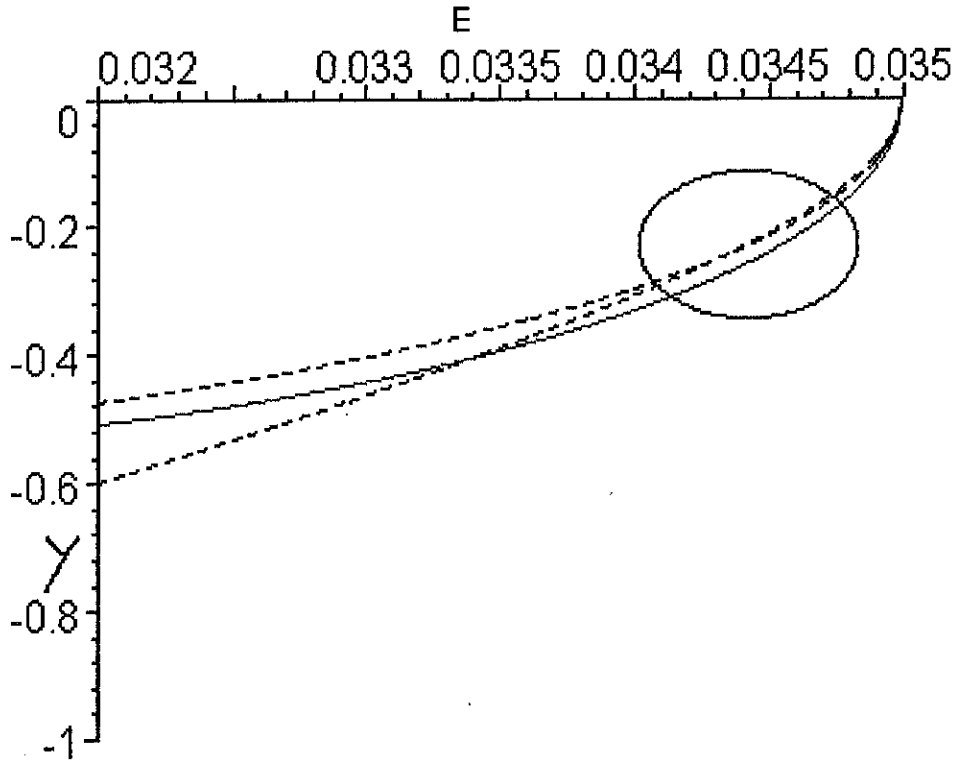

Figure 4.13: The last energy level of Figure 4.12 is magnified. Note that the second even solution occurs inside the oval.

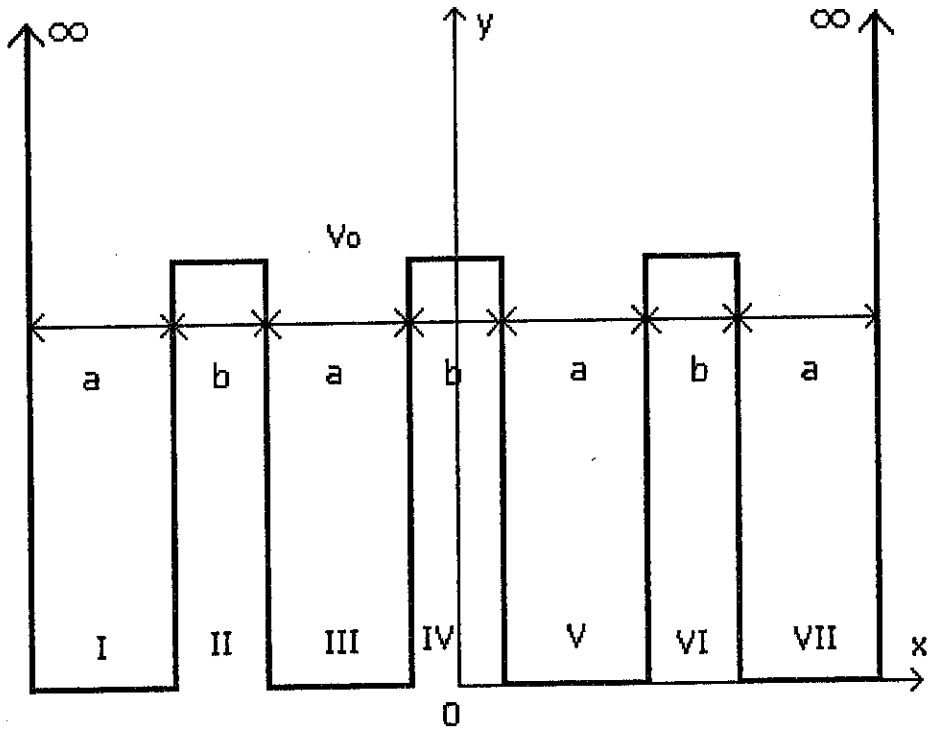

Figure 4.14: The potential is infinity at both end walls and V_0 at the top of the barrier. The width of a well is a and that of a barrier b.

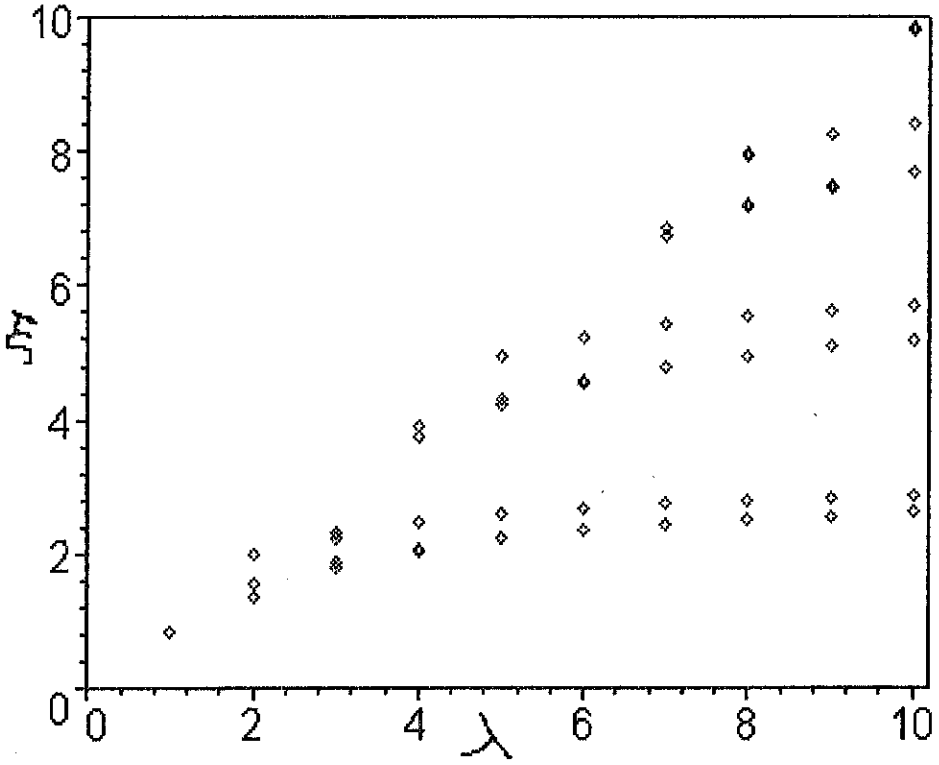

Figure 4.16: Convergence of Energy Solutions of the Symmetric Quadruple Well Potential when $\lambda = 10$.

On the other hand we know from symmetry about zero that the solution is either $F\cos(kx)$ or $F\sin(kx)$, where F is a constant, depending on even or odd, respectively. These solutions lead to quantization conditions.

For a double well potential we can find the ratio of A_1 and B_1 as

$$\frac{A_1}{B_1} = -e^{-3ika} \tag{4.63}$$

and since there is a barrier in the central domain, the wave function is either $G\cosh(qx)$ or $G\sinh(qx)$, where G is a constant, for even or odd solutions, respectively. The boundary conditions at the well-barrier interface lead to the elimination of G and to the energy quantization.

For a triple well potential,

$$\frac{A_1}{B_1} = -e^{-5ika} \tag{4.64}$$

$$\frac{C_2}{D_2} = -\frac{e^{-3qa}\left[\frac{A_1}{B_1}\left(\frac{ik}{q}+1\right)-e^{-3ika}\left(\frac{ik}{q}-1\right)\right]}{\frac{A_1}{B_1}\left(\frac{ik}{q}-1\right)-e^{-3ika}\left(\frac{ik}{q}+1\right)} \tag{4.65}$$

and we choose either $F\cos(kx)$ or $F\sin(kx)$ in the middle well and get quantization.

For a quadruple well potential, the ratios are

$$\frac{A_1}{B_1} = -e^{-7ika} \tag{4.66}$$

$$\frac{C_2}{D_2} = -\frac{e^{-5qa}\left[\frac{A_1}{B_1}\left(\frac{ik}{q}+1\right)-e^{-5ika}\left(\frac{ik}{q}-1\right)\right]}{\frac{A_1}{B_1}\left(\frac{ik}{q}-1\right)-e^{-5ika}\left(\frac{ik}{q}+1\right)} \tag{4.67}$$

depending on the middle well or barrier.

Therefore, for an N-well potential

$$\frac{A_1}{B_1} = -e^{-(2N-1)ika} \tag{4.78}$$

$$\frac{C_{2m}}{D_{2m}} = -\frac{e^{-[2N-(4m-1)]qa}\left[\frac{A_{2m-1}}{D_{2m-1}}\left(\frac{ik}{q}+1\right)-e^{-[2N-(4m-1)]ika}\left(\frac{ik}{q}-1\right)\right]}{\frac{A_{2m-1}}{B_{2m-1}}\left(\frac{ik}{q}-1\right)-e^{-[2N-(4m-1)]ika}\left(\frac{ik}{q}+1\right)} \tag{4.79}$$

$$\frac{A_{2m+1}}{B_{2m+1}} = \frac{e^{-[2N-(2(2m+1)-1)]ika}\left[\frac{C_{2m}}{D_{2m}}\left(\frac{ik}{q}+1\right)+e^{-[2N-(2(2m+1)-1)]ika}\left(\frac{ik}{q}-1\right)\right]}{\frac{C_{2m}}{D_{2m}}\left(\frac{ik}{q}-1\right)+e^{-[2N-(2(2m+1)-1)]qa}\left(\frac{ik}{q}+1\right)} \tag{4.80}$$

where m is an integer and $1 \leq m \leq \frac{N-2}{2}$ if N is even, or $1 \leq m \leq \frac{N-1}{2}$ if N is odd. $\frac{C_{2m}}{D_{2m}}$ and $\frac{A_{2m+1}}{B_{2m+1}}$ are sequentially repeated until $2m$ or $2m+1$ reaches $N-1$. Again, the last boundary condition gives quantization.

4.5 Accuracy and Dispersion of Quantum Clocks

All the potential models considered above are examples of clocks of very small size, great accuracy, and long running time. For a potential with N wells, we can construct N equally spaced energy levels as discussed above. We construct from the N different stationary states $\phi_1, \phi_2, \ldots, \phi_N$ a superposition representing the state of the clock wavefunction $\psi(t)$:

$$\psi(t) = \sum_{1}^{N} a_k \phi_k e^{-i\omega_k t} \tag{4.81}$$

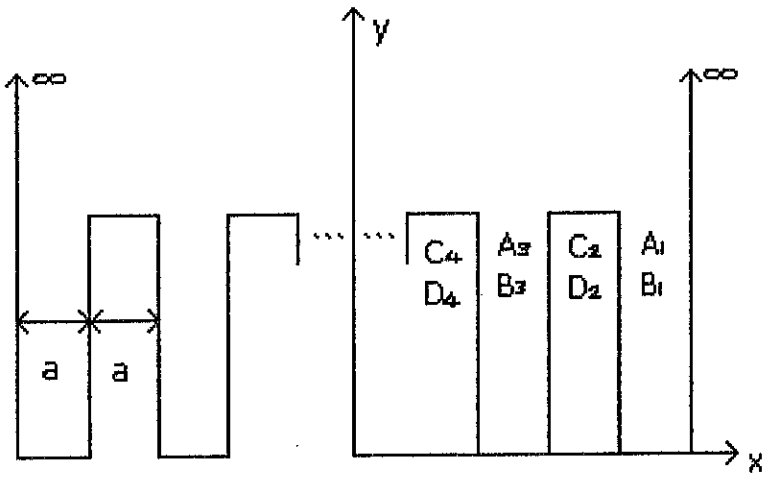

Figure 4.17: This is the multi well potential with the same widths 'a' for the well and the barrier. The wells are labeled A's and B's whereas the barriers C's and D's.

equation and that do not appear in previous discussions of quantum clocks. The first feature that appears naturally within Dirac theory is spin and the second is the existence of negative energy solutions.

The quantum clocks can be extended using special relativity [5, 14]. The quantum clocks mentioned so far are nonrelativistic devices which are used to study systems obeying nonrelativistic dynamics. Eventually, clocks should be constructed and operate in accordance with the postulates of relativity. For the purpose of this, a clock-interaction Hamiltonian in a Dirac equation should be considered and the explicit construction of a clock can be achieved by extending Salecker and Wigner's clock to include relativistic dynamics. In the following sections of this chapter, I briefly discuss the interaction of a relativistic particle with a clock and then I consider relativistic models for clocks based on single and double well potentials in Dirac theory.

5.2 A Dirac Particle and the Quantum Clock

The total Hamiltonian operator for the relativistic closed system (Dirac particle + clock) is in analogy with (3.11)

$$H = -i\,\alpha \cdot \nabla + \beta\, m_0 + P(q) H_c, \tag{5.1}$$

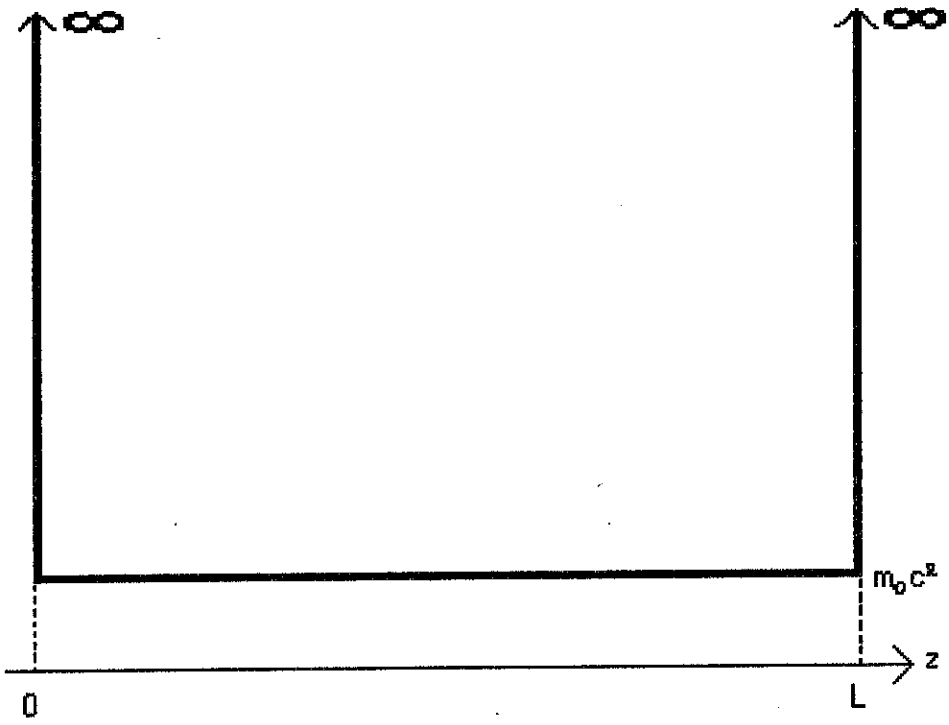

Figure 5.1: This is a relativistic single well potential. Potential is infinite at the end walls and m_0c^2 is the rest energy of a Dirac particle confined to the well potential.

When the particle moves in the positive z direction with momentum $\hbar k$, the normalized solution of the Dirac equation (5.4) [9, 12] is

$$\psi_k(z) = \sqrt{\frac{E + m_0c^2}{2m_0c^2}} e^{ikz} \begin{pmatrix} \chi \\ \frac{\sigma_z \hbar kc}{E+m_0c^2}\chi \end{pmatrix} \tag{5.5}$$

where $E = \sqrt{(\hbar kc)^2 + m_0^2c^4}$ is the energy of the relativistic particle and χ is an arbitrary normalized two-component spinor, i.e., $\chi^\dagger\chi = 1$. The spinor χ can be represented as $\chi = \begin{pmatrix} 1 \\ 0 \end{pmatrix}$ for spin 'up,' and as $\chi = \begin{pmatrix} 0 \\ 1 \end{pmatrix}$ for spin 'down,' or any linear combination of these two. Note that Equation 5.4 contains negative energy solutions as well, such as $E = -\sqrt{(\hbar kc)^2 + m_0^2c^4}$.

In non-relativistic quantum mechanics the vanishing of the wavefunctions at the end walls is a sufficient condition for finding eigenvalue solutions. However, in relativistic quantum mechanics, the boundary conditions are different from those in non-relativistic quantum mechanics because in relativistic quantum mechanics the wavefunction is a spinor of four complex components coupled in a system of first-order differential equations. The spinor cannot vanish at the boundaries of the infinite well potential because imposing this would make the wavefunction identically zero. In this case one can impose the fact that the flux of probability is continuous at the end walls of the potential. The wavefunction is not necessarily continuous however.

Therefore, the solution can be obtained by applying appropriate boundary

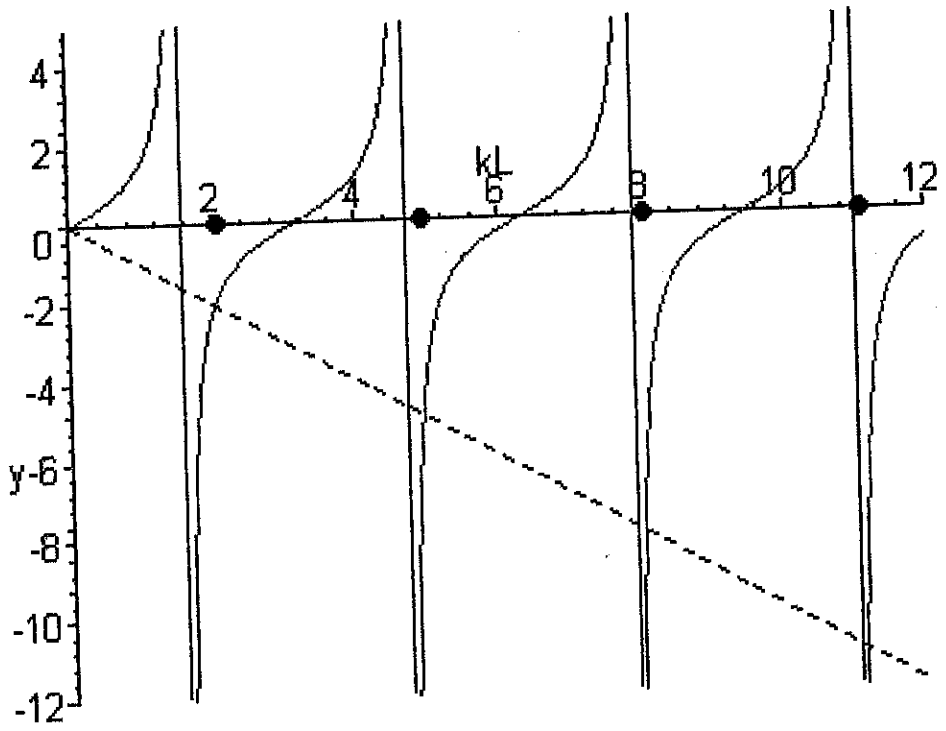

Figure 5.2: The function $\tan(kL)$(curve) and $-kL$(dotted line) are plotted separately when $L = \frac{\hbar}{m_0 c}$. The values of kL where the two functions intersect each other are the solutions. The dots on the horizontal axis are the reflections of the intersections. The roots are found at 0, 2.028757838, 4.913180439, 7.978665712 and 11.08553841.

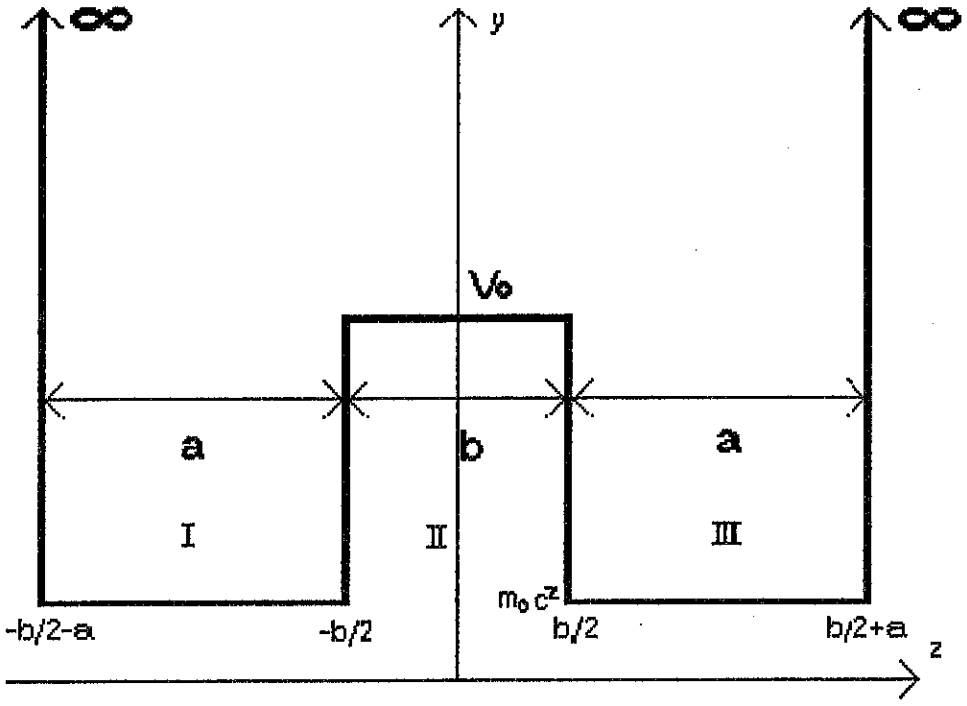

Figure 5.3: This one dimensional double well potential is symmetric with respect to its central vertical axis. The width of each of the potential well is a and that of the central barrier is b. The potential energy is V_0 at the top of the barrier, and m_0c^2 at the bottom of the potential well, where m_0 is the rest mass of a Dirac particle confined to the potential well and c is the speed of light. Three regions are distinguished, from left to right, 'Region I,' 'Region II,' and 'Region III.'

at the two end walls of the potential. Since no current flows through the end walls, (5.20) is the condition of impenetrability ($\vec{j} = 0$). On the contrary, the boundary conditions at the two inner potential walls are

$$\rho_I(-b/2) = \rho_{II}(-b/2) \tag{5.21}$$

$$\rho_{II}(b/2) = \rho_{III}(b/2) \tag{5.22}$$

and

$$\vec{j}_I(-b/2) = \vec{j}_{II}(b/2) \tag{5.23}$$

$$\vec{j}_{II}(b/2) = \vec{j}_{III}(b/2). \tag{5.24}$$

Note that at the inner walls the wavefunctions are continuous as well, just like in the Schrödinger case; therefore,

$$\psi_I(-b/2) = \psi_{II}(-b/2) \tag{5.25}$$

$$\psi_{II}(b/2) = \psi_{III}(b/2). \tag{5.26}$$

For ρ and $\vec{j}$ are constructed from ψ, (5.21), (5.22), (5.23), and (5.24) follow from (5.25) and (5.26).

Since $\vec{j} = c\psi^\dagger \vec{\alpha} \psi$,

$$j_{z\,I} = c\psi_I^\dagger \alpha_z \psi_I$$

$$= c\left[A^* e^{-ip_1 z/\hbar}\left(1,\ 0,\ \frac{p_1 c}{E + m_0 c^2},\ 0\right) + B^* e^{ip_1 z/\hbar}\left(1,\ 0,\ \frac{-p_1 c}{E + m_0 c^2},\ 0\right)\right] \times$$

$$\left(1-\frac{p_1^2c^2}{(E+m_0c^2)^2}\right)\left(A^*Be^{-2ip_1z/\hbar}+B^*Ae^{2ip_1z/\hbar}\right). \quad (5.30)$$

Similarly,

$$\rho_{II}=\left(1+\frac{p_2^2c^2}{(E+m_0c^2-V_0)^2}\right)(CC^*+DD^*)+$$
$$\left(1-\frac{p_2^2c^2}{(E+m_0c^2-V_0)^2}\right)\left(C^*De^{-2ip_2z/\hbar}+D^*Ce^{2ip_2z/\hbar}\right) \quad (5.31)$$

and

$$\rho_{III}=\left(1+\frac{p_1^2c^2}{(E+m_0c^2)^2}\right)(FF^*+GG^*)+$$
$$\left(1-\frac{p_1^2c^2}{(E+m_0c^2)^2}\right)\left(F^*Ge^{-2ip_1z/\hbar}+G^*Fe^{2ip_1z/\hbar}\right). \quad (5.32)$$

By the symmetry consideration (similar to the Schrödinger case discussed in Section 4.1, but in stead of ψ, ρ should be considered), parity equations can be written as

$$\rho_I(-z)=\rho_{III}(z) \quad (5.33)$$

$$\rho_{II}(-z)=\rho_{II}(z), \quad (5.34)$$

and from (5.20) and (5.33), we can find that $A=\pm G$ and $B=\pm F$, and from (5.34) $C=\zeta D$ where ζ is a real constant (I will find the possible value for ζ later). Therefore, (5.29) can be rewritten as

$$j_{z\,III}=\left(BB^*\frac{2p_1c^2}{E+m_0c^2}-AA^*\frac{2p_1c^2}{E+m_0c^2}\right) \quad (5.35)$$

By the symmetry of the well potential, it is enough to consider the boundary conditions only for the right half of the well potential. Then, the boundary condition for ρ at $z = \frac{b}{2}$ is from (5.22)

$$\left(1+\frac{p_2^2c^2}{(E+m_0c^2-V_0)^2}\right)(CC^*+DD^*)+$$
$$\left(1-\frac{p_2^2c^2}{(E+m_0c^2-V_0)^2}\right)\left(C^*De^{-ip_2b/\hbar}+D^*Ce^{ip_2b/\hbar}\right)$$
$$=\left(1+\frac{p_1^2c^2}{(E+m_0c^2)^2}\right)(AA^*+BB^*)+$$
$$\left(1-\frac{p_1^2c^2}{(E+m_0c^2)^2}\right)\left(B^*Ae^{-ip_1b/\hbar}+A^*Be^{ip_1b/\hbar}\right). \tag{5.41}$$

If we apply the MIT bag model boundary condition to ψ_{III} at $z = a + \frac{b}{2}$, then

$$-i\beta\,\alpha_z\psi_{III} = \psi_{III} \tag{5.42}$$

and we can find a relation between A and B as

$$B = A\frac{iP_1-1}{iP_1+1}e^{-2ik_1(a+b/2)} \tag{5.43}$$

where $P_1 = \frac{\hbar k_1 c}{E+m_0c^2}$ by using $p_1 = \hbar k_1$. Since P_1 is real, $\frac{iP_1-1}{iP_1+1}$ has unit modulus. So let

$$\frac{iP_1-1}{iP_1+1} = e^{i\delta} \tag{5.44}$$

where

$$\delta = \arctan\left(\frac{2P_1}{P_1^2-1}\right), \tag{5.45}$$

If we divide (5.53) by (5.52), then we have

$$\frac{CP_2e^{ik_2b/2} - DP_2e^{-ik_2b/2}}{Ce^{ik_2b/2} + De^{-ik_2b/2}} = \frac{2iFP_1e^{i\Gamma/2}\sin\left(\frac{k_1b}{2} + \frac{\Gamma}{2}\right)}{2Fe^{i\Gamma/2}\cos\left(\frac{k_1b}{2} + \frac{\Gamma}{2}\right)} \tag{5.54}$$

and (5.54) can be rewritten as

$$\frac{(C-D)P_2\cos\left(\frac{k_2b}{2}\right) + i(C+D)P_2\sin\left(\frac{k_2b}{2}\right)}{(C+D)\cos\left(\frac{k_2b}{2}\right) + i(C-D)\sin\left(\frac{k_2b}{2}\right)} = iP_1\tan\left(\frac{k_1b}{2} + \frac{\Gamma}{2}\right). \tag{5.55}$$

Since the right-hand side of (5.55) is purely imaginary, the relations between C and D that make the left-hand side of (5.55) purely imaginary as well are only $C = D$ and $C = -D$. Thus, if $C = D$, $\psi_{II}(z)$ becomes

$$\psi_{II}(z) = Ce^{ik_2z}\begin{pmatrix}\chi\\ P_2\chi\end{pmatrix} + Ce^{-ik_2z}\begin{pmatrix}\chi\\ -P_2\chi\end{pmatrix} \tag{5.56}$$

$$= C\begin{pmatrix}(e^{ik_2z} + e^{-ik_2z})\chi\\ P_2(e^{ik_2z} - e^{-ik_2z})\chi\end{pmatrix} \tag{5.57}$$

$$= C\begin{pmatrix}2\cos(k_2z)\chi\\ 2iP_2\sin(k_2z)\chi\end{pmatrix} \tag{5.58}$$

and if $C = -D$, $\psi_{II}(z)$ becomes

$$\psi_{II}(z) = Ce^{ik_2z}\begin{pmatrix}\chi\\ P_2\chi\end{pmatrix} - Ce^{-ik_2z}\begin{pmatrix}\chi\\ -P_2\chi\end{pmatrix} \tag{5.59}$$

$$= C\begin{pmatrix}(e^{ik_2z} - e^{-ik_2z})\chi\\ P_2(e^{ik_2z} + e^{-ik_2z})\chi\end{pmatrix} \tag{5.60}$$

$$= \left(1 - \frac{V_0}{E + m_0c^2}\right) \tan\left(\frac{\delta}{2} - \xi\right) \tag{5.69}$$

$$= \left(1 - \frac{V_0}{E + m_0c^2}\right) \tan\left(\frac{1}{2}\arctan\left(\frac{2P_1}{P_1^2 - 1}\right) - \xi\right) \tag{5.70}$$

$$= \left(1 - \frac{V_0}{E + m_0c^2}\right) \tan\left(\frac{1}{2}\arctan\left(-\frac{\hbar k_1}{m_0 c}\right) - \xi\right), \tag{5.71}$$

where $\xi = k_1 a$, $\eta = k_2 a$ and $\frac{2P_1}{P_1^2 - 1} = -\frac{\hbar k}{m_0 c}$.

Similarly, if $C = -D$, we have

$$\cot\left(\frac{\eta}{2}\right) = -\left(1 - \frac{V_0}{E + m_0c^2}\right) \tan\left(\frac{1}{2}\arctan\left(-\frac{\hbar k_1}{m_0 c}\right) - \xi\right). \tag{5.72}$$

By using $p_1 c = \hbar k_1 c = \sqrt{E^2 - m_0^2 c^4}$ and $p_2 c = \hbar k_2 c = \sqrt{(V_0 - E)^2 - m_0^2 c^4}$, (5.71) and (5.72) become

$$\tan\left(\frac{a\sqrt{(V_0 - E)^2 - m_0^2 c^4}}{2\hbar c}\right) = \left(1 - \frac{V_0}{E + m_0c^2}\right) \times \tan\left(\frac{1}{2}\arctan\left(-\frac{\sqrt{E^2 - m_0^2 c^4}}{m_0 c^2}\right) - \frac{a\sqrt{E^2 - m_0^2 c^4}}{\hbar c}\right) \tag{5.73}$$

$$\cot\left(\frac{a\sqrt{(V_0 - E)^2 - m_0^2 c^4}}{2\hbar c}\right) = -\left(1 - \frac{V_0}{E + m_0c^2}\right) \times \tan\left(\frac{1}{2}\arctan\left(-\frac{\sqrt{E^2 - m_0^2 c^4}}{m_0 c^2}\right) - \frac{a\sqrt{E^2 - m_0^2 c^4}}{\hbar c}\right), \tag{5.74}$$

and by introducing a factor $\Omega = \frac{E}{V_0}$, (5.73) and (5.74) can be rewritten as

$$\tan\left(\frac{aV_0\sqrt{(1 - \Omega)^2 - \frac{m_0^2 c^4}{V_0^2}}}{2\hbar c}\right) = \left(1 - \frac{1}{\Omega + \frac{m_0 c^2}{V_0}}\right) \times$$

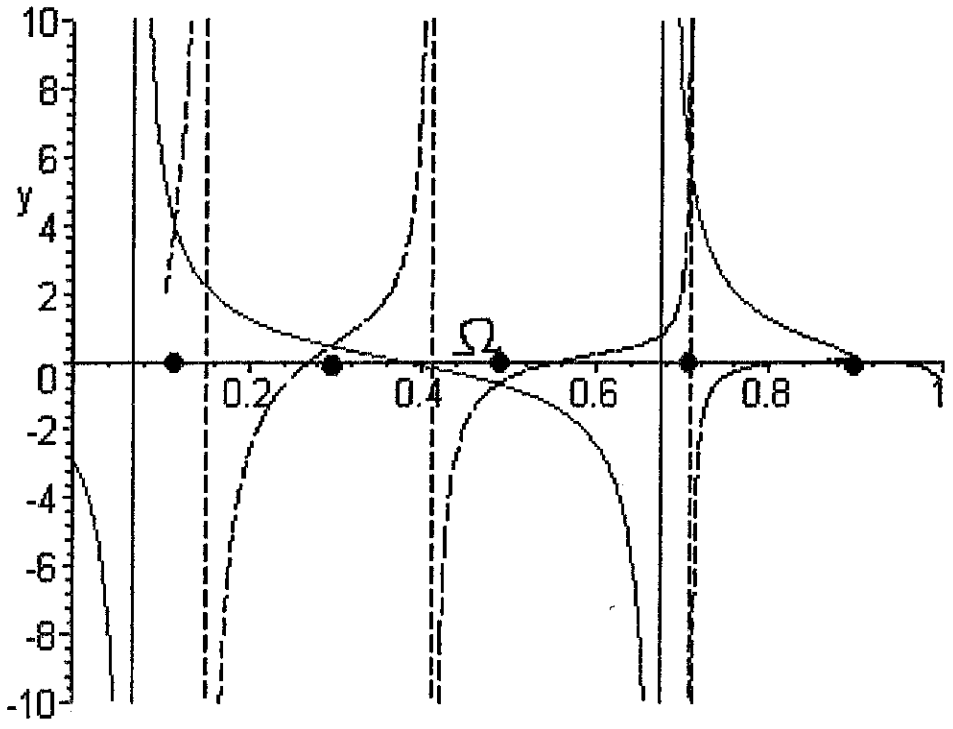

Figure 5.4: The plot of (5.75) when $a = 0.004\mathring{A} = 4.0 \times 10^{-13}m$, $V_0 = 5MeV$. The solid curve is for the left-hand side of the equation and the dotted line for the right-hand side of the equation. The intersections are the values of Ω which are projected on the horizontal axis (big dots). They are from the smallest one 0.1146732981, 0.2936768933, 0.4872453509, 0.7063278448 and 0.9000000000.

These equations are just a first step toward the general solution of the double well problem. Our study is limited to the spin 'up' case, one-dimensional motion, and energy ranges such that $E > m_0c^2$ and $|V_0 - E| > m_0c^2$. However, we believe that the more general cases can be constructed using the results developed in this chapter without too many difficulties.

wavefunction be zero makes the wavefunction vanish everywhere. This is similar to the impossibility of imposing boundary conditions on ψ and ψ' simultaneously in the Schrödinger case. Thus, the substitution for the boundary condition is that the current or flux is zero at the wall of the infinite potential well, and that the probability density is continuous.

I have explored the possibility of a ticking quantum clock by studying various square well potentials. However, a perfect quantum clock will not be built soon. There are still several obstacles to be overcome to produce a working quantum clock.

First, I considered only one-dimensional well potentials, and the ideal well potentials are square-shaped. Real systems are neither one-dimensional nor square-shaped. Moreover, they interact with their surroundings. Note also that for the relativistic quantum clock, I neglected special relativistic effects between frames such as time dilation which is associated with fast moving particles. However, if we use an approximation method such as WKB [13], we can study quantum clocks that are more realistic. This task can probably be done by cooperation between physicists and quantum engineers. Microscopic multi-well structures can now essentially be built to any particular specification [15].

The second obstacle is the inherent limitation on the resolution of a quantum clock that was pointed out not only by Salecker and Wigner but also by Peres. So

tum mechanics after all. But for the concepts of time, I have to remind myself of St. Augustine as quoted in my introduction, "What is time?–if nobody asks me, I know; but if I try to explain it to one who asks me, I do not know" [10].

[10] *Physics and the Ultimate Significance of Time*, edited by D. R. Griffin, (Albany: State University of New York, 1986).

[11] H. Hellman, *Great Feuds in Science*, (New York: John Wiley & Sons, 1998).

[12] R. H. Landau, *Quantum Mechanics II*, (New York: John Wiley & Sons, 1996).

[13] R. L. Liboff, *Introductory Quantum Mechanics*, (New York: Addison-Wesley, 1992).

[14] S. N. Mayburov, Los Alamos Preprint quant-ph/9801075, (30 Jan, 1998).

[15] G. J. Milburn, *Schrödinger's Machines*, (New York: Freeman and Company, 1997).

[16] J. von Neumann, *Mathematical Foundations of Quantum Mechanics*, (Princeton: Princeton University, 1955).

[17] D. Park, *Fundamental Questions in Quantum Mechanics*, edited by L. M. Roth and A. Inomata (Albany: State University of New York, 1984), pp.263–78.

[18] A. Peres, Am. J. Phys. **48**, 552 (1980).

[19] H. Salecker and E. P. Wigner, Phys. Rev. **109**, 571 (1958).

[20] S. F. Savitt, *Time's Arrows Today*, (New York: Cambridge University Press, 1995).